ONR21
LTR-90-001

Final Report
AGILE MULTIPLE APERTURE IMAGER RECEIVER DEVELOPMENT

Prepared by:

David E.B. Lees and Robert F. Dillon

Prepared for:

Office of Naval Research
Code 12613
800 N. Quincy Street
Arlington, VA 22217-5000

Contract No. N00014-89-C-0200

15 February 1990

"Research supported by the Strategic Defense Initiative/
Innovative Science and Technology and managed
by the Office of Naval Research."

SPARTA INC.
24 Hartwell Avenue
Lexington, MA 02173
(617)863-1060

UNCLASSIFIED

SECURITY CLASSIFICATION OF THIS PAGE

REPORT DOCUMENTATION PAGE

1a. REPORT SECURITY CLASSIFICATION UNCLASSIFIED	1b. RESTRICTIVE MARKINGS
2a. SECURITY CLASSIFICATION AUTHORITY	3. DISTRIBUTION/AVAILABILITY OF REPORT
2b. DECLASSIFICATION/DOWNGRADING SCHEDULE	
4. PERFORMING ORGANIZATION REPORT NUMBER(S) LTR90-001	5. MONITORING ORGANIZATION REPORT NUMBER(S)
6a. NAME OF PERFORMING ORGANIZATION SPARTA INC. — 6b. OFFICE SYMBOL (If applicable)	7a. NAME OF MONITORING ORGANIZATION Office of Naval Research
6c. ADDRESS (City, State, and ZIP Code) 24 Hartwell Avenue Lexington, MA 02173	7b. ADDRESS (City, State, and ZIP Code) 800 N. Quincy Street Arlington, VA 22217-5000
8a. NAME OF FUNDING/SPONSORING ORGANIZATION Strategic Defense Initiative — 8b. OFFICE SYMBOL (If applicable) T/IS	9. PROCUREMENT INSTRUMENT IDENTIFICATION NUMBER N00014-89-C-0200
8c. ADDRESS (City, State, and ZIP Code) The Pentagon Washington, D.C. 20301-7100	10. SOURCE OF FUNDING NUMBERS PROGRAM ELEMENT NO. — PROJECT NO. — TASK NO. — WORK UNIT ACCESSION NO.

11. TITLE (Include Security Classification)

Agile Multiple Aperture Imager Receiver Development

12. PERSONAL AUTHOR(S)
David E.B. Lees and Robert F. Dillon

13a. TYPE OF REPORT	13b. TIME COVERED	14. DATE OF REPORT (Year, Month, Day)	15. PAGE COUNT
Final Report	FROM 8/15/89 TO 2/14/90	2/13/90	40

16. SUPPLEMENTARY NOTATION

17. COSATI CODES			18. SUBJECT TERMS (Continue on reverse if necessary and identify by block number)
FIELD	GROUP	SUB-GROUP	

19. ABSTRACT (Continue on reverse if necessary and identify by block number)

A variety of unconventional imaging schemes have been investigated in recent years that rely on small, unphased optical apertures (subaperture) to measure properties of an incoming optical wavefront and recover images of distant objects without using precisely figured, large-aperture optical elements. Such schemes offer several attractive features. They provide the potential to create very large effective apertures that are expandable over time and can be launched into space in small pieces. Since the subapertuers are identical in construction, they may be mass producible at potentially low cost.

This final report presents a preliminary design for a practical low-cost optical receiver The multiple aperture design has high sensitivity, wide field-of-view, and is light-weight. A combination of spectral, temporal, and spatial background suppression are OVE used to achieve daytime operation at low signal levels. Modular packaging to make the —

20. DISTRIBUTION/AVAILABILITY OF ABSTRACT ☐ UNCLASSIFIED/UNLIMITED ☒ SAME AS RPT. ☐ DTIC USERS	21. ABSTRACT SECURITY CLASSIFICATION UNCLASSIFIED
22a. NAME OF RESPONSIBLE INDIVIDUAL	22b. TELEPHONE (Include Area Code) — 22c. OFFICE SYMBOL

DD FORM 1473, 84 MAR — 83 APR edition may be used until exhausted. All other editions are obsolete.

SECURITY CLASSIFICATION OF THIS PAGE
UNCLASSIFIED

19. ABSTRACT (cont.)

number of receiver subapertures conveniently scalable is also presented. The design is appropriate to a ground-based proof-of-concept experiment for long-range active speckle imaging.

Accession For	
NTIS GRA&I	☑
DTIC TAB	☐
Unannounced	☐
Justification	
By per telecon	
Distribution/	
Availability Codes	
Dist	Avail and/or Special
A-1	

STATEMENT "A" per Mr. W. Micell
ONR/Code 12613-Boston
TELECON 3/1/90 CG

TABLE OF CONTENTS

1 Executive Summary 1

2 Introduction to Multiple Aperture Imaging 6

3 Strawman Experiment 8

4 Receiver Requirements 12

5 Receiver Design 15

5.1 Design Logic 15

5.2 Collection Optics 19

5.3 Mechanical Scanner. 21

5.4 Subaperture Detector 24

5.5 Array Electronics 25

5.6 Receiver Packaging 29

6 Receiver Performance and Cost 36

7 Conclusions 38

8 References 39

1 Executive Summary

This final report presents the results of a Phase I SBIR program titled "Agile Multiple Aperture Imager Receiver Development." The purpose of this work was to examine the feasibility of building a ground-based multiple aperture receiver intended for long-range imaging proof-of-concept experiments. The three key questions identified in the Phase I proposal were as follows:

1. What are the performance requirements for a multiple aperture receiver designed to operate in a ground-to-space imaging experiment?
2. Can a receiver be designed using existing component technologies to meet these requirements and, if so, what would the design look like?
3. If a suitable design exists, are the risk and cost associated with its implementation low enough to be practical?

The Statement of Work to address these questions consisted of technical tasks plus final report production:

1. *Configure Strawman Experiment.* Generate (to first order) a strawman imager geometry based on intensity interferometry that is suitable for imaging space objects from the ground. Establish the system wavelength, expected range to target, target sizes, receiver array geometry, etc.
2. *Develop Receiver Requirements.* Based on the strawman system concept, bound the values of the critical receiver performance parameters.
3. *Survey Technology/Preliminary Receiver Design.* Generate a preliminary receiver design that achieves the performance requirements determined in Task 2. Survey existing component technologies (e.g. detectors, spectral filters, low-cost optical elements) and refine the design to minimize production costs and enhance performance.
4. *Estimate Receiver Performance and Cost.* Estimate the value of each critical receiver parameter based on the known performance of components elected for the design. This includes estimating the cost to mass-produce the subapertures in quantities ranging from 100 to 10,000 units.

SPARTA answered the three key questions during the course of Phase I and accomplished several major milestones as a result. First, receiver performance requirements were identified for a strawman ground-to-space multiple aperture imager (MAI) experiment. Second, a concept for a practical, low-cost subaperture receiver was identified by eliminating a large number of competing schemes. Third, a candidate subaperture array packaging scheme was identified which potentially accommodates receiver testing, adjusting, and repairing while supporting coarse array steering, easy array expansion and long-term mechanical pointing stability.

A Phase II proposal has been submitted to SDIO for fabrication and testing

of sample hardware. The proposed effort will eliminate all remaining technical and most of the remaining cost risks associated with the receiver. This will clear the way for the sponsor's decision to fund fabrication of a small (32×32) to moderately-sized (64×64) array for MAI validation experiments.

Key receiver performance requirements were established for a strawman ground-to-space MAI experiment based hypothetically at ISTEF near Kennedy Space Center in Florida. These requirements are summarized in Table I. Three significant conclusions should be noted. The subaperture must operate in the photon-noise limited mode at signal levels approaching 10 photons/sample to meet the equivalent noise input requirement. Secondly, the combination of spatial, spectral, and temporal background suppression mechanisms must operate very effectively or the background suppression requirements will not be met. Finally, a single subaperture and its electronics must be buildable at low cost or the concept quickly becomes impractical in cost.

Table I. Receiver performance requirements for strawman experiment.

Parameter	Nominal Value
Operating Wavelength	0.5-0.65 μm
Quantum Efficiency	$\geq$ 0.05
Equivalent Noise Input	$\leq$ 1 photoelectron
Dynamic Range	$\geq$ 1000:1
Electrical Bandwidth	$\geq$ 1.0×10^7 Hz
Aperture Diameter	$\approx$ 5 cm
Max. Package Width	$\simeq$ 10 cm
Total Field of View (FOV)	$\pm$ 10°
Instantaneous Field of View (IFOV)	$\approx$ 1 mrad
IFOV Slew Rate	$\geq$ 10 rad/sec
IFOV Settling Time	$\leq$ 50 msec to 0.1% of FOV
Max. Sky Background	$\approx$ 100 W/sr $-$ m^2 $-$ μm
Background Suppression	$\leq$ 2.0×10^{-16} sr $-$ s $-$ μm
Max. Cost per Subaperture	$\leq$ \$4,000

The subaperture design is illustrated in Figure 1. It consists of a collection lens, a crossed-slit focal plane scanner assembly, a spectral filter and polarizer combination, and a low-cost, high-gain photomultiplier tube. The focal plane scanner provides the combination of high spatial background rejection and agile

IFOV steering required for day-time operation. Incorporating a photomultiplier tube as the detector element provides low noise, high gain, high sensitivity, and high electrical bandwidth at a very low cost (a few hundred dollars).

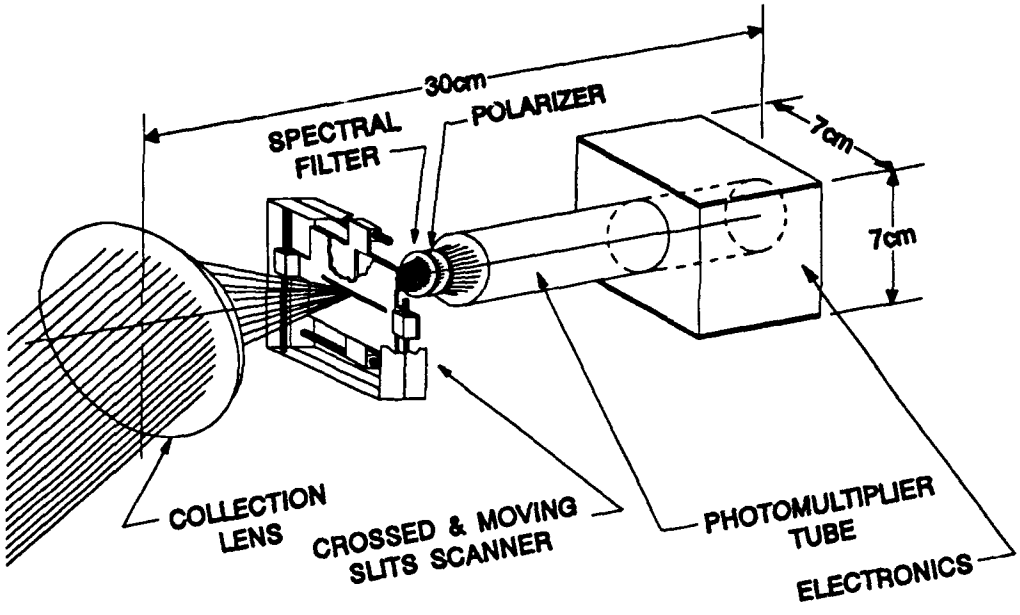

Figure 1. Low-cost subaperture design concept.

We propose to package subapertures in 8 × 8 "subarrays" to facilitate coarse steering, array expansion, and array repair. The proposed subarray mechanical structure is illustrated in Figure 2. This overall approach can pack subapertures together at a minimum center-to-center spacing equal to the collection lens diameter plus about 25 mm. Consequently, it will accommodate the baseline design of 5 cm diameter subapertures spaced 10 cm apart. A metal base plate fabricated using aluminum, carbon composite laminates, or some other lightweight, low-cost, and stiff material will serve as the interface to a coarse azimuth-elevation gimbal. It will also act as the platform upon which additional mounting hardware is placed. A series of vertical support plates will be attached to the baseplate using a number of identical angle brackets as shown. These vertical plates will be fabricated from the same material used for the baseplate, insuring matched thermal expansion properties. All vertical plates (eight per subarray) will be identical in design to facilitate low-cost manufacturing. The interfaces between the angle brackets, vertical plates and baseplate will be secured using dowel pins and screw fasteners. Consequently, the vertical plate spacing can be changed by simply drilling, reaming, and tapping a series of holes in the baseplate. No complex milling or machining will be required.

The remainder of this report provides a detailed technical summary of the

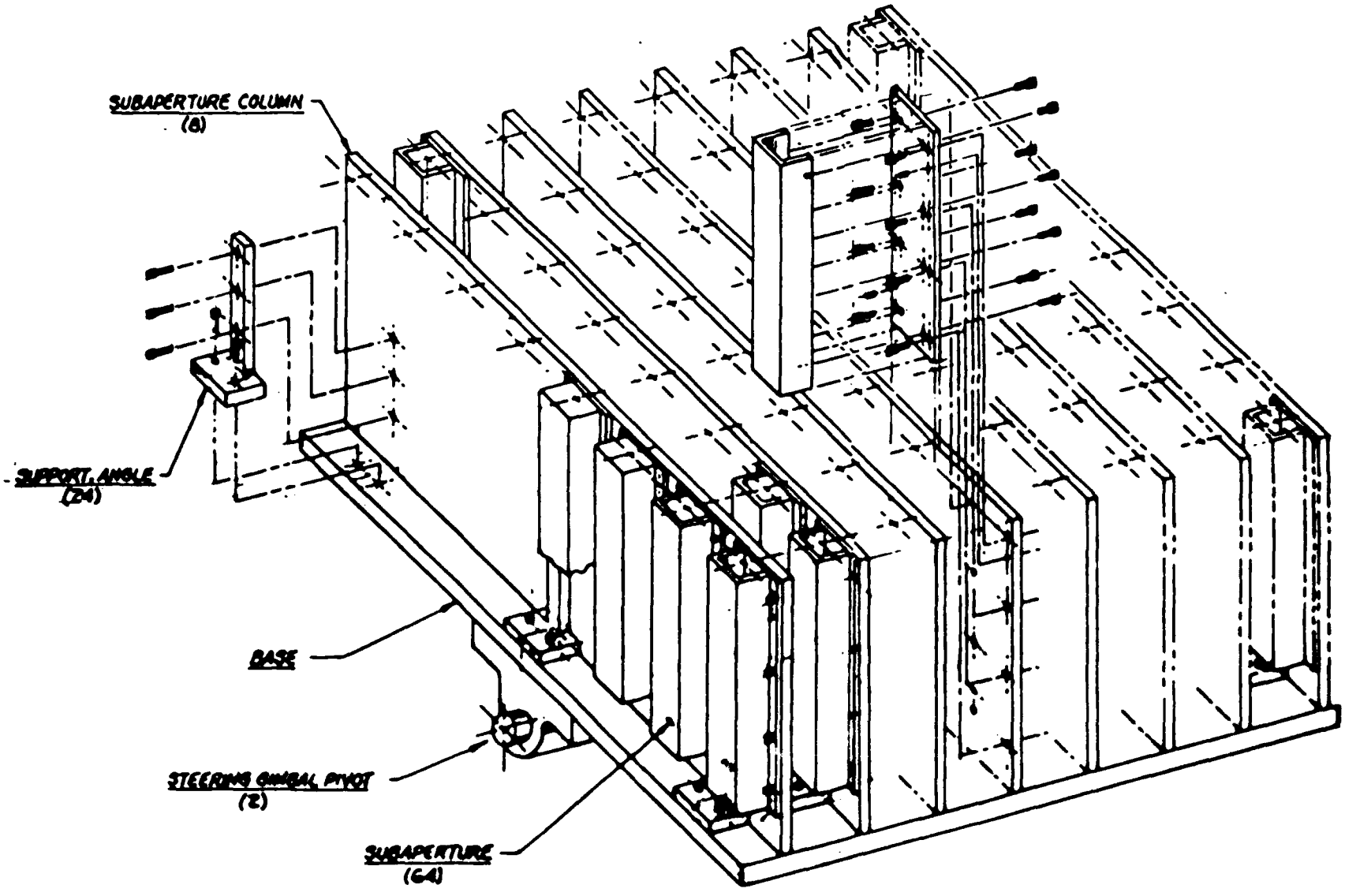

Figure 2. Subaperture array packaging concept.

Phase I accomplishments. Section 2 provides the reader with background information on the multiple aperture imaging concept that can utilize the receiver being discussed. Sections 3 through 6 discuss the strawman experiment configuration, resulting receiver requirements, receiver design, and projected receiver performance and cost, respectively. Section 7 lists general conclusions drawn from our Phase I work. References are included as Section 8.

2 Introduction to Multiple Aperture Imaging

Active optical systems have potential for both long range discrimination and pointing and tracking missions. The narrow beamwidth and high angular resolution of optics provide advantages which can make optics the sensor of choice for these missions.

Angle-angle images can be used to make several measurements which are useful for discrimination. Relative tracking of objects released from a PBV provides plume interaction information, which can be used to distinguish heavy objects from light objects. Shape and shape change information is useful for discriminating cheap inflatable balloon and replica decoys. In each of these cases, the availability of image information provides additional information about the targets. This information may be useful to eliminate the possibility of simple countermeasures which could fool a non-imaging sensor.

Angle-angle images are required for guidance and scheduling of directed energy weapons. These missions include aimpoint determination and damage/kill assessment. Aimpoint algorithms may require determination of object position, velocity, and orientation. Image information can be used to perform centroiding to achieve an accurate measurement of target angular position. The effects of transient glints and coherent speckle phenomena can be overcome by the use of intensities in multiple pixels.

The large aperture required to achieve high angular resolution presents several problems for conventional optical systems. For imaging with sub-meter resolution at a range of several thousand kilometers, apertures greater than one meter in diameter are required. Apertures of this size are difficult to steer rapidly to image 20 or more targets per second. In addition, fabrication of large primary mirrors is more difficult for large aperture sizes. Finally, the weight of large mirrors must scale approximately as D^3 to maintain the mirror figure without active correction, and weight equals cost for a space-based system. Active correction requires complex control systems and a beacon or other means for determining correct actuator position.

The solution to the problems of fabricating and steering extremely large primary mirrors is to divide the large aperture into many smaller subapertures. The problem then becomes one of combining the outputs of the subapertures to produce an image (or other target signature).

There are several approaches to combining the signals from each subaperture. For example, if the amplitude and relative phase in each subaperture are known, then the image can be calculated using a single Fourier transform. Direct measurement of phase, however, requires a structure with stability of a fraction of a

wavelength over the entire aperture. SPARTA and others have extensively investigated the multiple aperture imaging concept[1-7] illustrated in Figure 3. With this concept, we have chosen to perform direct detection and recover the phase information using phase retrieval and the well-known properties of coherent speckle. The use of direct detection in each subaperture means that the apertures need not be phased to a fraction of a wavelength and greatly simplifies array construction. The use of direct detection also simplifies each subaperture and means that an "electronically-agile" receiver can be built by staring at a large field-of-view and performing effective background suppression. This imager concept has been demonstrated through simulation and bench-top experiments.

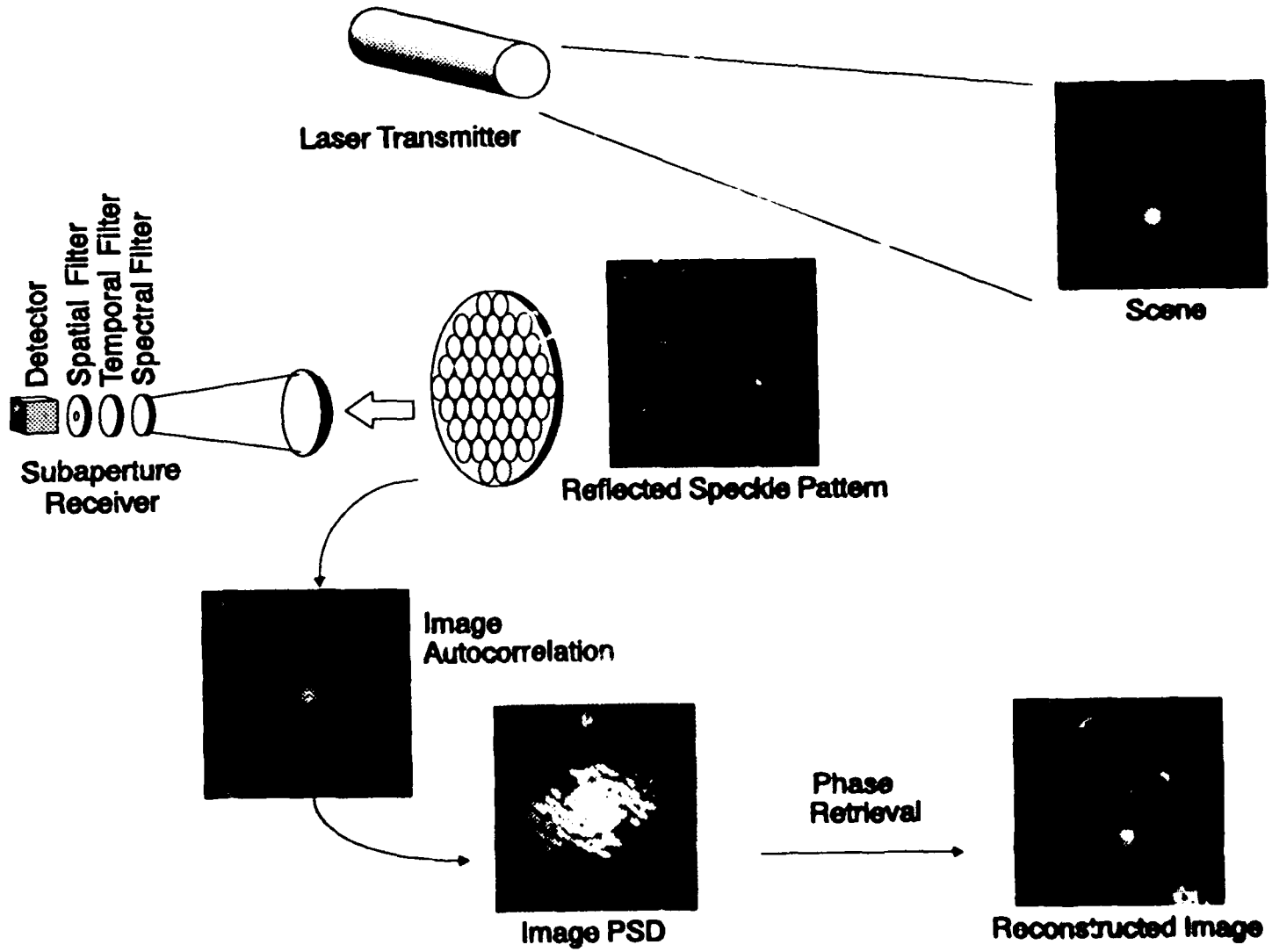

Figure 3. SPARTA's Multiple Aperture Imager Concept.

3 Strawman Experiment

This section discusses the configuration of the strawman experiment which determined the parameter values of our multiple aperture receiver. This work corresponds to Task 1 of our Phase I Statement of Work. The results of this investigation were a set of system parameters summarized in Table I of Section 1.

A strawman experiment based on the 1984 Optical Discrimination Study[8] (ODS) was used for target mission parameters. The ODS concluded that 20 to 50 targets per second had to be imaged at ranges of several thousand kilometers with submeter resolution. For the purpose of the Phase I effort it was assumed a 10 cm resolution at ranges greater than 100 km is required for a target with linear dimension of one meter.

The subaperture attenuation and sky radiance must be considered in any ground-based experiment. LOWTRAN 7 was used for atmospheric modeling. The LOWTRAN model was setup for a midlatitude, maritime atmosphere, with a spring-summer troposphere extinction coefficient height profile at the coordinates of Cape Kennedy. Figures 4 and 5 plot spectral radiance and atmospheric transmission respectively as a function of wavelength. Both radiance and transmission curves show that receiver wavelength for a ground-based experiment should be done at longer visible or near IR wavelengths. A wavelength range of 0.5-0.65 μm is chosen based on likely laser and detector components.

The sun was at its noon-time position on day 180 of the year. For an active imaging system light must travel from the transmitter to the target and back to the receiver making two passes through the atmosphere. Thus, the square of the atmospheric transmission to space is plotted against elevation angle in Figure 6 for an atmospheric visibility of 23 km and in Figure 7 a visibility of 10 km. This curve was generated for an illumination wavelength of 500 nm. The two-way transmission falls below ten percent at 28 degrees with 23 km visibility and 48 degrees above the horizon for 10 km visibility. It is desirable to conduct experiments above elevation angles of 30 degrees, even on clear days or atmospheric transmission losses will make signal levels too low.

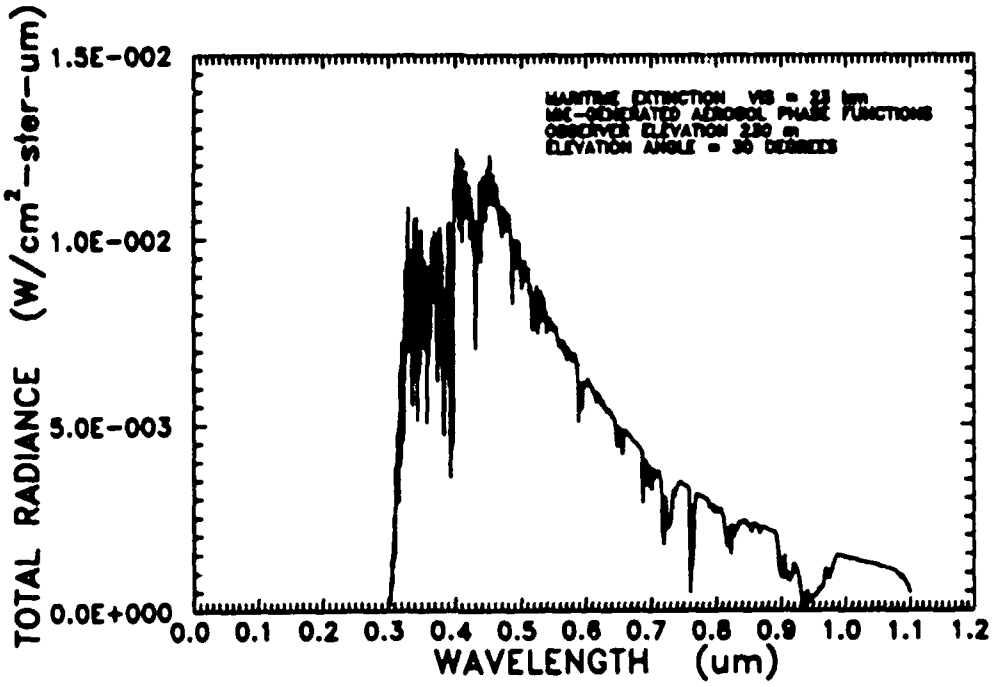

Figure 4. Midsummer standard clear day sky spectral radiance.

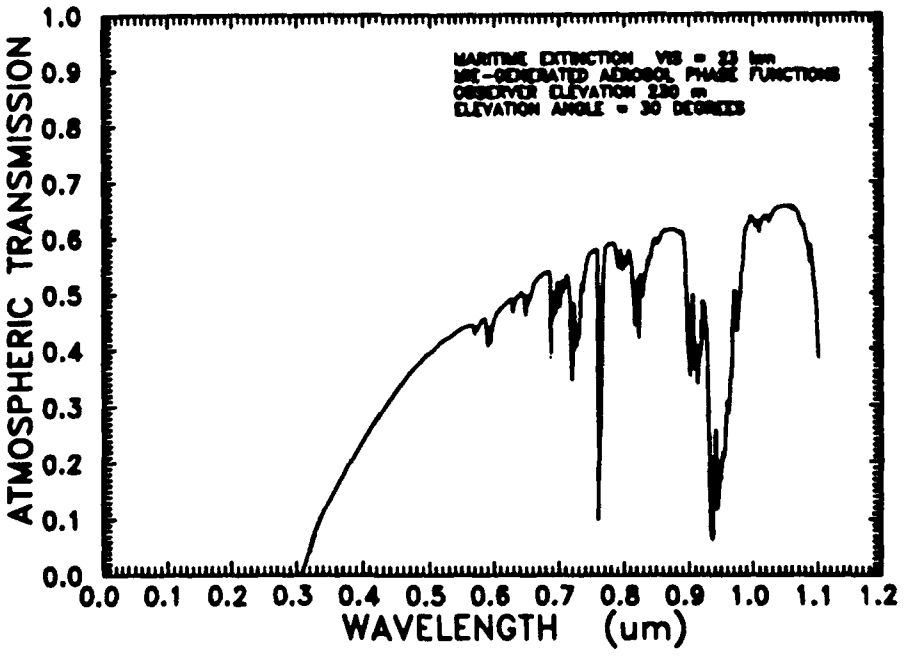

Figure 5. Midsummer standard clear day sky one-way transmission to space.

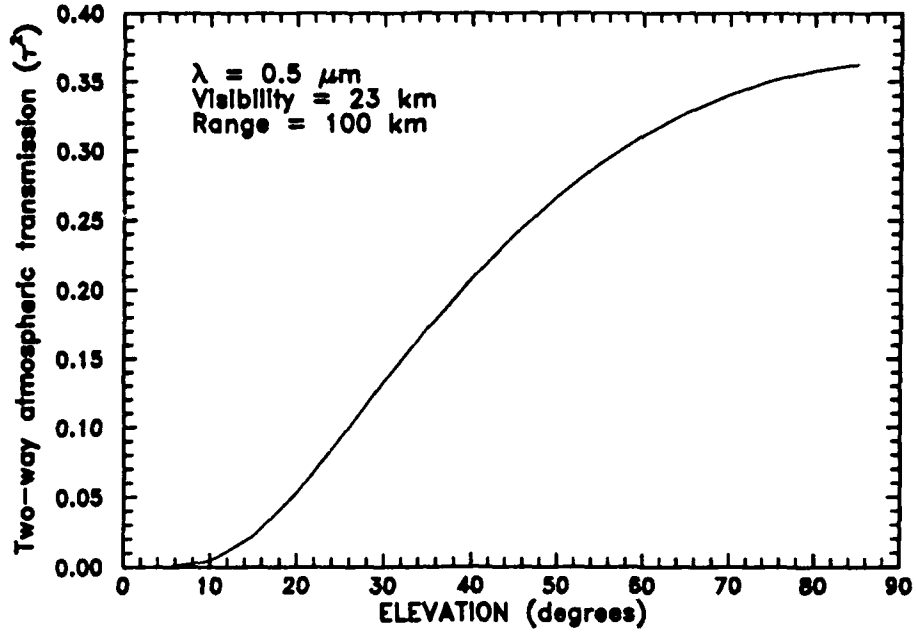

Figure 6. Two-way atmospheric transmission to space on a standard clear day.

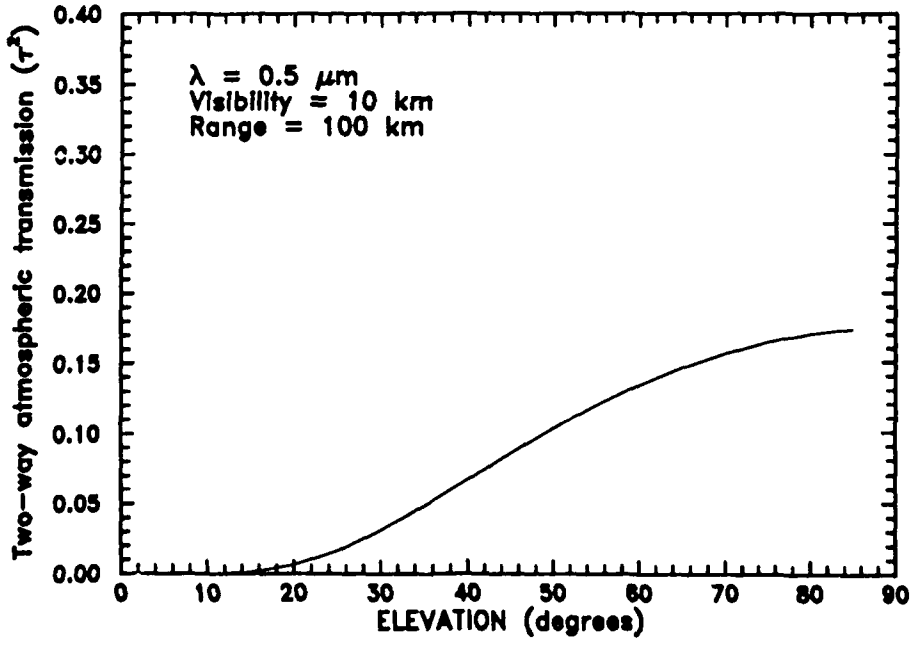

Figure 7. Two-way atmospheric transmission with light haze.

4 Receiver Requirements

In this section receiver requirements will be bounded based on the strawman experiment parameters. The work described in this section corresponds to Task 2 of our Phase I Statement of Work. The results of this work set clear bounds on the sensitivity and background suppression capability required for each subaperture.

The signal levels for the strawman mission require a very low light level detector. Assuming a circular receiver field-of-view, targets which backscatter light uniformly into 2π steradians, uniform transmitter illumination of a circular area, and a linear polarizer in the receiver, the number of signal photons is given by the expression

$$N_s \approx (\frac{E_t}{h\nu})(T)\left(\frac{A_t}{A_i}\right)(\rho)\left(\frac{D^2}{16R^2}\right)$$

where

N_s = number of signal photons arriving at each subaperture detector,

E_t = transmitter energy,

T = two-way atmospheric transmission,

ρ = target reflectivity,

D = receiver diameter,

A_t = target cross section,

A_i = area illuminated, and

R = range to target.

Substituting order of magnitude estimates for each term in parentheses and assuming a one joule laser operating in the middle of the visible spectrum with a target at 250 km, the number of signal photons, N_s, is approximately

$$N_s \approx 10^{19} \times 10^{-1} \times 10^{-1} \times 10^{-1} \times (\frac{10^{-1}}{10^6})^2 \approx 100 \text{ photons.}$$

The maximum operating range for the multiple aperture imager is determined by subaperture background suppression. It can be shown that for a given mission (i.e., constant imaging resolution, illuminated area, and target properties) the return signal is range-independent. The background, on the other hand, can be shown to scale linearly with range for a given mission because the supaperture size grows to keep the resolution and signal strength constant. Thus, the amount of background suppression in a subaperture determines the maximum operating range.

In order to estimate background and signal levels at the detectors it is necessary to assume a subaperture spacing and diameter. For example, assume it is desired

to achieve 10 cm imaging resolution for the strawman experiment presented above. This means the subapertures are spaced 10 cm apart. Further, assume a 50 percent linear fill factor to limit spatial averaging of the speckle [9] (and improve receiver MTF) so that the collection optics have a 5 cm diameter entrance pupil.

The next issue is to estimate background levels. LOWTRAN 7 was used to estimate sky spectral radiance, N_{sky}, on a standard clear day (visibility of 23 km) looking 30 degrees above the horizon at noontime. Additionally, we assumed Mie scattering through a maritime aerosol atmosphere with an observer altitude of 230 meters above sea level. The background was normalized to a 5 cm circular aperture and expressed in photons/(s − sr − μm).

The background radiance is a strong function of wavelength, as shown in Figure 8. For example, the normalized sky spectral radiance decreases from 1.8×10^{17} to 1.0×10^{17} photons/(s − sr − μm) when the wavelength changes from 0.5 to 0.7 μm. From a background standpoint, operation at longer wavelengths is desirable. The sky radiance is a function of many atmospheric parameters and can vary by a factor of five depending on exact conditions, so the sky background curve should be considered a "ballpark" estimate.

The term "background suppression" can now be quantitatively defined as S,

$$S \equiv \theta^2 \Delta\lambda \, \tau,$$

where

θ = instantaneous full field-of-view,

$\Delta\lambda$ = spectral filter bandwidth, and

τ = detector integration time.

Given the suppression and sky radiance, the number of background photons N_b, that reach the detector is computed as

$$N_b = N_{sky} S.$$

Since signal levels will be tens to hundreds of photons, the background should be limited to tens of photons to maintain a reasonable signal-to-noise ratio. Assuming the strawman requirements of a 5 cm diameter subaperture, sky spectral radiance of 100 w/(sr − m^2 − μm) and a wavelength of 0.5 μm, the required background suppression to limit background on the detector to 100 photons is 2×10^{-16} sr − s − μm. The definition of background suppression suggests three

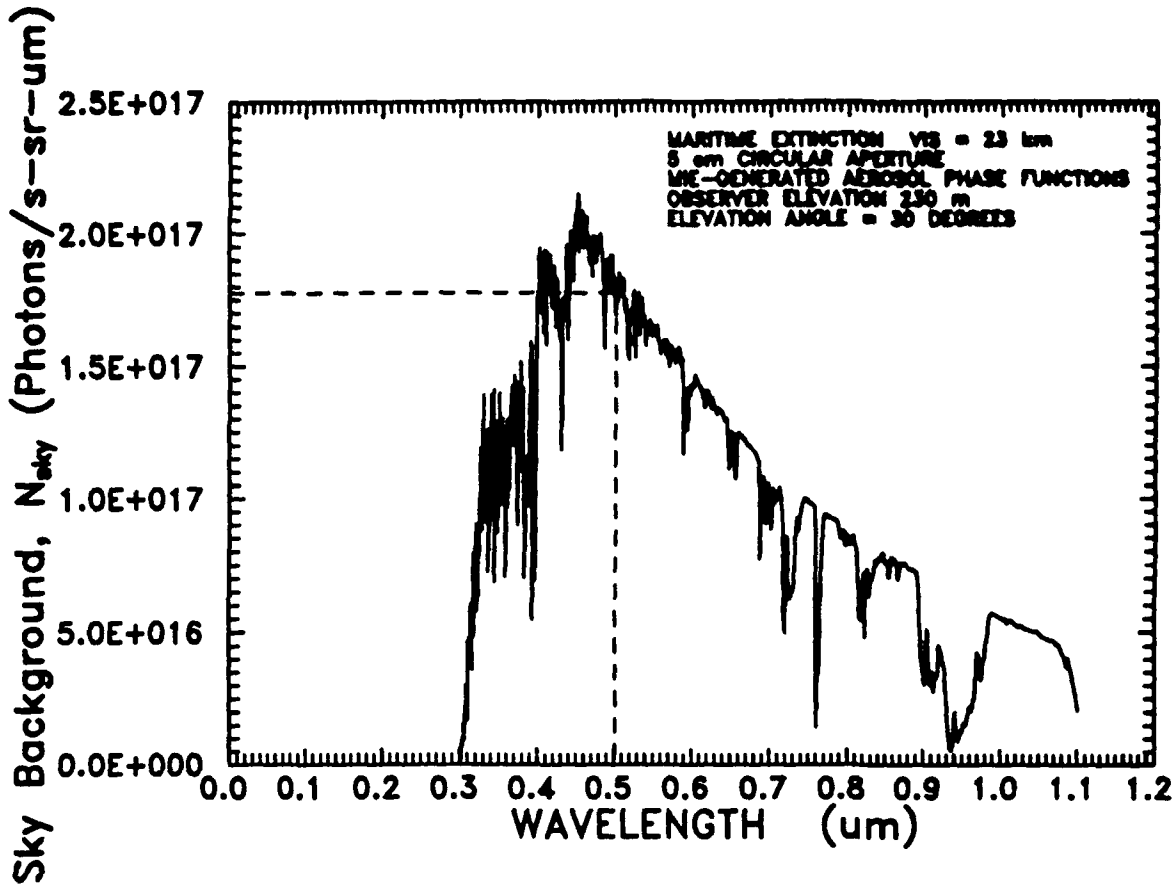

Figure 8. Normalized sky spectral radiance.

methods to reduce background: spectral, temporal and spatial background suppression. Each of these methods will be considered in turn in the receiver design section.

5 Receiver Design

In this section we will show how the design constraints determined by cost, return signal strength, range to target and background irradiance narrow the subaperture configurations to a single concept. Each constraint and its influence on system design will be discussed in turn. Based on these constraints, we have developed a preliminary design for each major element of the system: collection optics, mechanical scanner, subaperture detector, electronics, and array packaging. The development of the preliminary design presented in this section was Task 3 of our Phase I Statement of Work.

The constraints on the design determined by cost, background suppresion requirements, and sensitivity are presented in this section. These constraints lead to a *single* workable subaperture design.

5.1 Design Logic

The cost constraint is driven by a goal of $5M total cost for the receiver subaperture array. Typical systems will have one to four thousand subapertures. This restricts the cost per subaperture for all parts and assembly. Thus, all subaperture components must be low cost and simple.

It has been shown that day-time background suppression requirements are large so three different methods of background suppression will now be considered.

Spectral suppression uses an optical bandpass filter to reduce the number of background photons that are not at the laser illuminator wavelength. The Doppler shift for space targets is on the order of 0.1 nm which means the maximum spectral suppression is $10^{-4}\mu$m. It is possible to achieve this narrow bandwidth over a 20 degree field-of-view (full angle) using Lyot-type birefringent filters[10], but they are very expensive (several thousand dollars) and often require active temperature control to maintain constant wavelength. Given the cost constraints on the subapertures, Lyot filters are not a good choice. Conventional interference-type bandpass filters can be built with the desired bandpass (0.1 nm), but they exhibit too much angle shift to be operated over a 10 degree half angle. The minimum bandwidth for a visible wavelength interference filter operating over the desired field of view is about 2 nm. Such filters deliver a spectral suppression of $2 \times 10^{-3}\mu$m, which is an order of magnitude larger than optimal, but at a price ($\approx$ $20) in line with the goal of a low cost subaperture.

The temporal component of suppression is simply the detector integration time. By ranging the object being imaged, the receiver can be turned on only during the time window when the backscattered signal falls on the receiver. This reduces background photons and detector noise. Assuming object range is known within

15 meters, a 100 nanosecond integration time will not cut out any signal and will offer a suppression of 10^{-7} seconds.

The combination of spectral and temporal suppression supplies about $2 \times 10^{-10}\mu$m-sec as a suppression factor. The third method for background suppression is limiting the portion of the sky instantaneously viewed by the receiver. Figure 9 plots required IFOV (Instantaneous Field Of View) for a circular field of view versus normalized sky radiance assuming the background must be reduced to 10 photons. The first major conclusion from this plot is that night-time operation over a 20 by 20 degree field-of-view can be achieved with only spectral and temporal suppression. This is very important, because it means a *night-time imager can be operated with no spatial agility required.* The second conclusion is that operation in the middle of the day will require an IFOV on the order of a milliradian, and this will need to be rapidly steered to cover 340 milliradians (20 degrees).

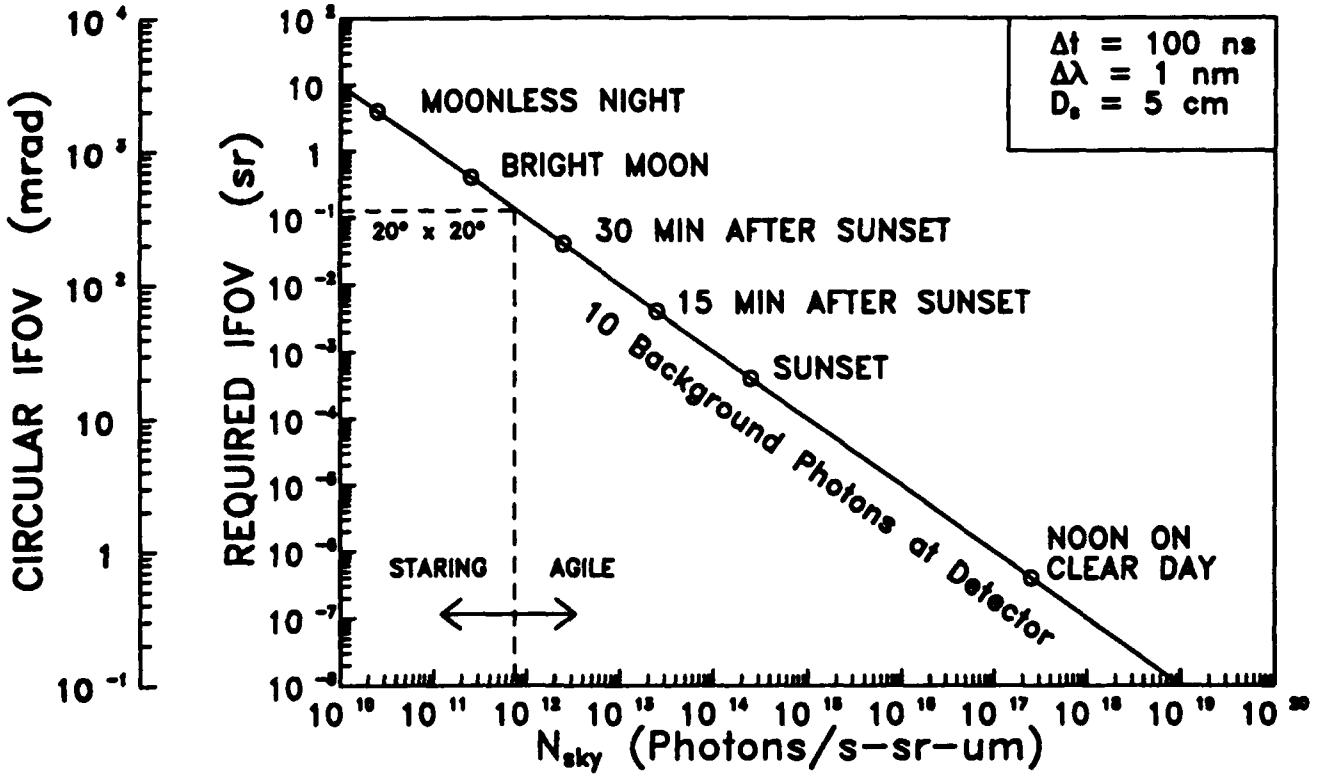

Figure 9. Required IFOV vs. sky radiance.

The design of a day/night subaperture has been shown to require spatial agility for day-time operation. This means a small field of view must be steered over a 20 degree full angle in less than 50 milliseconds. The two basic scanning methods

are pupil plane and focal plane. In pupil plane scanning the optical system has a small IFOV which is steered by changing the angular orientation of a mirror in front of the collection optics. Unfortunately, there are several serious problems with pupil plane scanning. The first is the packaging requirement for a two-axis, large-aperture scanner. The strawman system uses 5 cm apertures with 10 cm spacing which is hard to achieve because of motor-mirror geometry. The second problem is that the speed-power requirements are difficult to achieve because rigid mirrors with clear apertures larger than 5 cm must be moved very rapidly. The alternative to *pupil plane scanning* is *focal plane scanning*. The IFOV is steered by moving a small aperture in front of a large detector. In principle, focal plane scanning can be accomplished with no moving parts using a solid-state spatial light modulator. Unfortunately, solid-state SLMs tend to be too expensive and have insufficient contrast for background suppression. The contrast requirements for a focal plane scanner are very high. The required spatial suppression is on the order of 10^{-6} sr which implies that in a low light level system, the contrast ratio of the focal plane scanner must be better than 10^6 or the detector signal will be dominated by background noise. Mechanical focal plane scanning, on the other hand, can be accomplished by moving a very thin, low-mass, opaque plate containing a small aperture.

The combined requirements of background suppression, IFOV steering speed, and cost imply *mechanical focal plane scanning* using a small aperture in an opaque flat plate. In order to achieve two dimensional IFOV steering, it is proposed that a pair of slits move at right angles and be placed nearly on top of one another as shown in Figure 10. This design permits the use of low cost, reliable, high-speed, linear motors which have been developed for magnetic and optical disk technology.

There are four important detector requirements: large area to allow focal plane scanning, low noise because of the low signal levels, sufficient bandwidth to handle the required integration time, and low cost. A 35 mm diameter detector is required to cover the focal plane when a 5 cm diameter, F/2 collection optic is operated over a 20° FOV. The detector dark current should be much less than the average signal strength, so dark current must be less than 1 photoelectron per received pulse. The minimum detector bandwidth is set by the 100 ns required integration time. While a *minimum* bandwidth of 10 MHz is required, a 50 MHz bandwidth is desired for a practical system. Finally, any detector chosen must be low cost, with an upper bound of about $1000 to keep overall subaperture cost less than $4000 (worst case). Table II shows each of these four factors for five different candidate detectors. The only acceptable detector by these criteria is a photomultiplier tube.[11,12] Avalanche photodiodes are attractive because they are solid-state, batch-fabricated devices, but they are small area devices (typically a square millimeter) and will not cover the 35 mm diameter required for focal plane scanning.[13,14] Silicon

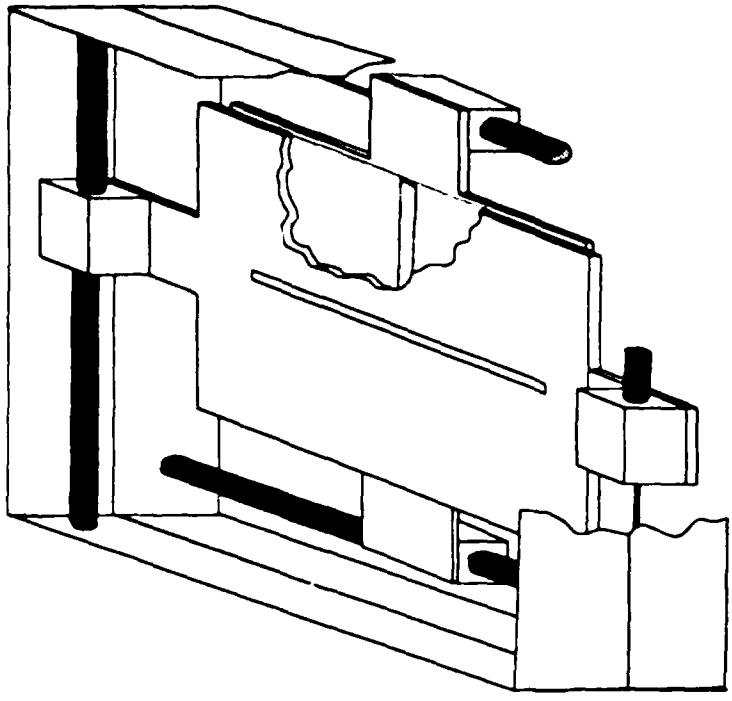

Figure 10. Two-dimensional, crossed-slit, mechanical focal plane scanner concept.

photodiodes[15] are low cost, large area, and moderate bandwidth devices (with large area), but they have too high a dark current to be useful for very low light level detection. Cooled CCD arrays offer low noise and large area, but they are very expensive[16] (more than $10,000) and typically have integration times in the millisecond range (using mechanical shutters). Microchannel plate charge amplifiers[17] used with CCD arrays allow short integration times by electronically switching the microchannel plate, but they are too expensive for the proposed work.

Table II. Detector requirements and candidate devices.

Detector	High Bandwidth	Low Noise	Low Cost	Large Area
Photomultiplier tube	√	√	√	√
Avalanche photodiode	√	√		
Silicon photodiode	√		√	√
Cooled CCD		√		√
MCP/CCD		√		√

After considering the above-mentioned physical and design constraints during

Phase I, a *single* workable subaperture design emerged. It is illustrated in Figure 11. The main subassemblies are an optical collection system, a mechanical focal plane scanner, a photomultiplier tube detector, and electronics. Each subassembly can be constructed using mature component technologies. Most of the components are available off the shelf and at low cost. Key components making up the subaperture will be discussed in this section.

5.2 Collection Optics

Lens design is an important part of the subaperture design. A diffraction-limited lens generates a blur circle with angular diameter

$$\beta = \frac{2.44\lambda}{D}$$

where λ is wavelength and D is the clear aperture. This means that for $\beta =$ 0.5 μm and $D = 5$ cm, a diffraction-limited system has an angular blur of 0.024 milliradians which is about 40 times smaller than the required one milliradian IFOV for day-time background suppression. Unfortunately, in a system with a minimal number of optical elements operating over a moderately large field of view (20 degrees full angle), geometric aberrations dominate. A single-element collection lens with spherical surfaces is desirable. The equations for geometrical aberrations (in radians) of a single-element lens bent to minimize spherical aberration are:

$$\text{spherical} = \frac{n(4n-1)}{128(n+2)(n-1)^2(F/\#)^3}$$

$$\text{sagittal coma} = \frac{\theta}{16(n+2)(F/\#)^2}$$

$$\text{astigmatism} = \frac{\theta}{2(F/\#)}$$

$$\text{sagittal field curvature} = \frac{\theta^2(n+1)}{(F/\#)2n}$$

$$\text{tangential field curvature} = \frac{\theta^2(3n+1)}{(F/\#)2n}$$

where n is the lens index of refraction, $F/\#$ is the lens F/number and θ is the angular field of view. Table III gives angular geometric aberration-induced blur (in milliradians) for a single element made of high index glass (SF6 with $n_d =$ 1.8) operated up to 10° off axis with lens bending (choice of first and second surface curvatures) chosen to minimize spherical aberration. Spherical aberration becomes acceptable (less than 1 mr) for an F/4 lens, but astigmatism is more than 21 mr. Even an F/20 system has astigmatism that is far too large. The conclusion from this table is that astigmatism and field curvature dominate and create blur spots several times larger than the required IFOV even for very slow

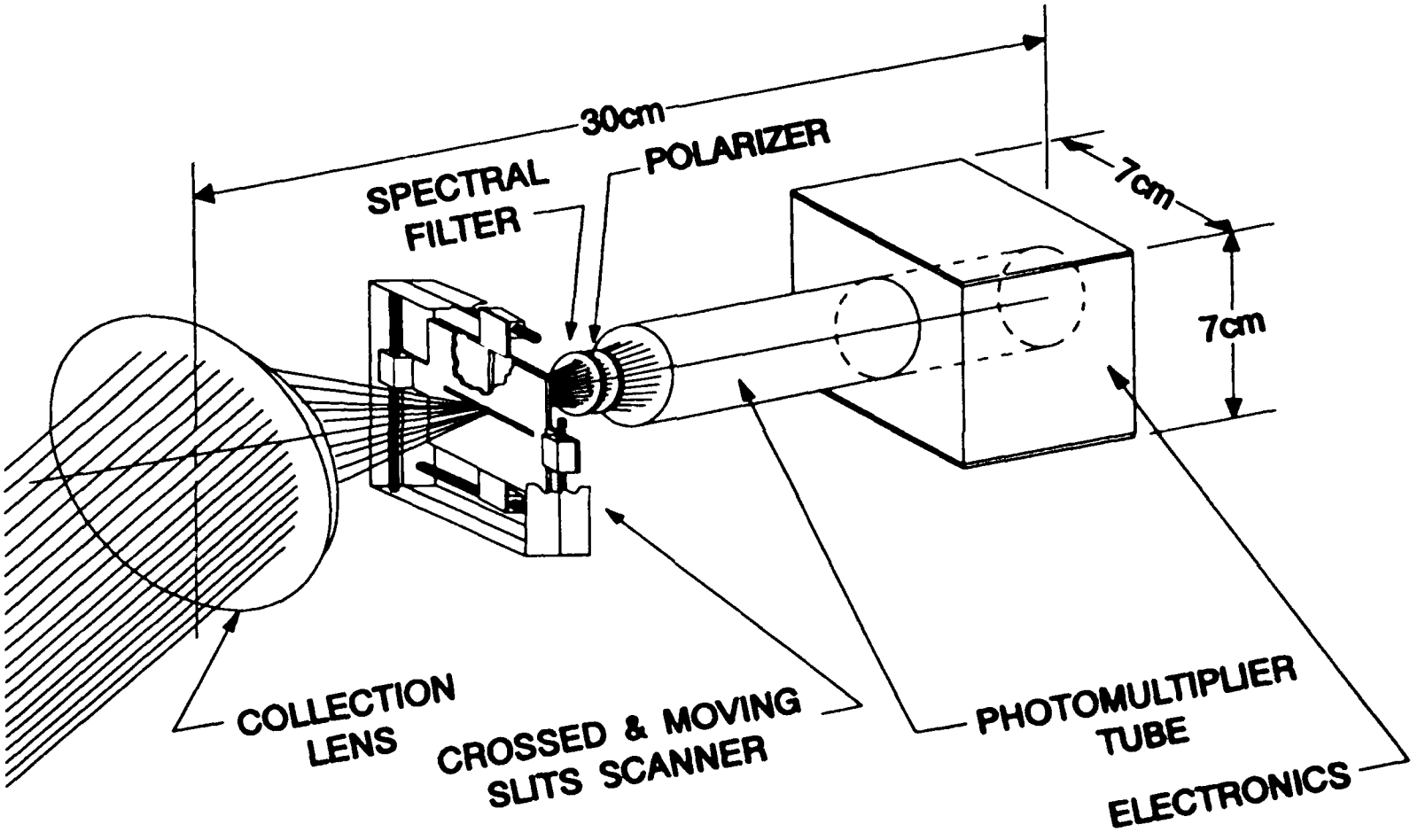

Figure 11. Subaperture design concept.

optical systems. Aspherizing a singlet can be used to eliminate spherical and coma but field curvature remains. Since a flat focal plane is required, it is clear that either a multielement or holographic lens design is required. A three-element Cooke triple can meet the field flatness requirements, for example.

Table III. Aberration blur (in milliradians) vs. lens F/number for an SF6 singlet with bending to minimize spherical aberration.

F/number	Sph.	Coma	Astig.	Field curve$_{sag.}$	Field curve$_{tang.}$
2	4.5	0.7	43.6	11.8	27.1
4	0.6	0.2	21.8	5.9	13.5
10	0.0	0.0	8.7	2.4	5.4
20	0.0	0.0	4.4	1.2	2.7

The overall length of the system is determined primarily by the optical system. A sunshade will be placed in front of the collection optics to restrict the background field of view to a cone with a 10 degree half angle. The need for internal baffling on the sunshade will be evaluated as part of the optical design. The sunshade/lens can be designed to function as a telecentric system, but unfortunately it is telecentric on the image side, so that little increase in depth of focus results.

Light scatter from any source is a serious design issue that will be addressed during the proposed work. Scatter can come from thin film coatings, collection lens elements, and internal mounts and flanges. Bulk scatter in a typical optical glass (BK7) is 10^{-6} cm^{-1} at 500 nm, which is a very serious background source in a wide-angle system. Furthermore, other types of common glasses have bulk scattering an order of magnitude larger than BK7. It is desirable from a scattering standpoint to operate at longer wavelength, since Rayleigh scattering scales as the fourth power of wavelength. Thin film anti-reflection and bandpass coatings can exhibit considerable scatter. For example, state of the art, low-scatter coatings have scatter of several parts per million. Since background must be reduced to 10 photons, the maximum full field of view over which a subaperture will work in daylight may turn out to be restricted by scattering.

The optical design tasks that must be done to build a subaperture are as follows. A complete optical design must be conducted using a lens design code with an optimizer. In addition, a careful evaluation of scattering sources must be done. This includes measuring the scatter from various components as described in the testing section. The number of optical elements must, of course, be minimized to hold down production fabrication costs. It is expected that two complete design cycles will be necessary. The design and testing are closely tied together, since component tests will be used to modify the design.

5.3 Mechanical Scanner.

Figure 4 shows a conceptual sketch of the mechanical scanner. The scanner consists of a pair of linear motors. Each motor moves a thin opaque aperture plate containing a narrow slit. The slit is attached to a pair of mounts which ride low friction rails. The motor/aperture assemblies are placed so that the slits move along orthogonal paths. The aperture plates must be thin and move close to one another. The collection lens depth of focus determines the thickness of the scanner aperture plates. The depth of focus is approximately equal to $fF/\#\beta$ where f is the focal length, F/# is the F-number of the lens, and β is maximum acceptable angular blur. In this case the instantaneous field of view is the maximum acceptable blur. For a 10 cm focal length, F/2 lens the depth of focus is about 200 μm. The depth of focus must be traded off against total scan distance. From the standpoint of placing crossed slits close together, it is desirable to make the optical system slower. For a constant entrance pupil diameter, the depth scales linearly with F/number. Unfortunately, the distance which a scanning slit must move to cover a constant angular field also scales linearly with F/number. Thus, doubling the depth of focus increases the scanning plate area by a factor of four.

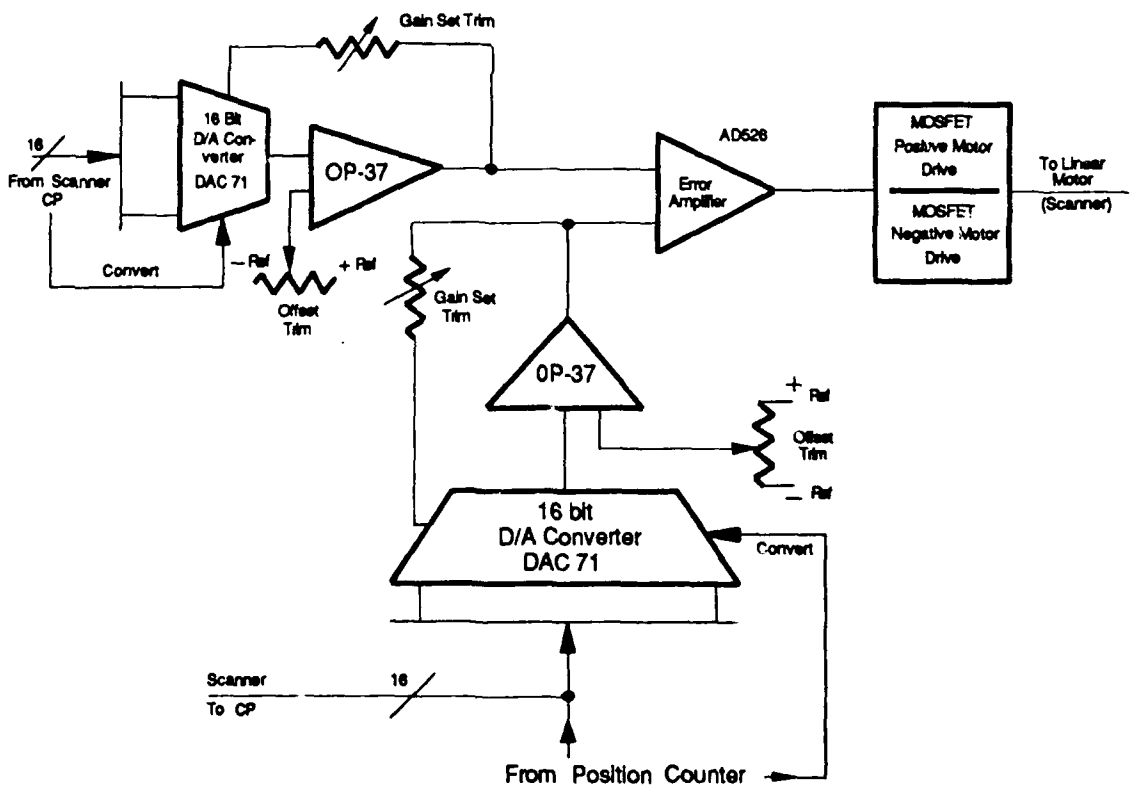

Figure 12. Analog driver for linear motor scanner.

The system requirement of steering to 20 targets per second forces a 50 millisecond maximum random access positioning time on the linear motor. This time is on the same order as typical optical and magnetic disk head positioning systems. Such systems have been built relatively cheaply and with MTBF exceeding 40,000 hours. Our positioning accuracy requirements, which are on the order of $\pm 10\mu m$, are much lower than those for disk head positioning. High speed motor technology is well developed and mature and should be readily transferable to subaperture fabrication.

A custom motor will be required because of the combination of cost, size, speed, and aperture mounting requirements. Feedback will be used to accurately position the aperture. An optical linear encoder will be built into each motor to accurately position it. The motor requirements are given in Table IV. The goal for motor cost, including the linear bearings and guides, is $150 (100-unit quantities) to keep the system cost within the prescribed limits.

Table IV. Target linear motor specifications.

QUANTITY	SPECIFICATION
Total travel distance	40 mm
Positioning accuracy	±0.01 mm over 35 mm ±0.5 mm over last 5 mm
Maximum positioning time	40 milliseconds over 35 mm travel
Aperture mass	5 grams
Aperture plate dimensions	40 by 80 mm

The scanner motor electronic drivers must be able to source and sink a large amount of current to enable high slew rate operation and ensure positional accuracy. The strawman scanner must be able to slew 35 mm and achieve a positional accuracy of $\pm 10\mu m$. The scanner position sensing will be done using absolute count from a home position. On power up, the scanners will be at "home" position. Attached to each scanner section (x and y) will be a linear (quadrature) encoder. The output from the encoder will be fed into comparators to square the waveforms, then to a logic array consisting of a "D" flip-flop and a 16-bit counter. The "D" flip-flop will be set if the scanner is moving away from home and reset if the scanner moves towards home. The output of the flip-flop controls the count direction of the counter. The counter value represents the absolute position of the scanner assembly.

The motor driver consists of three basic parts as shown in Figure 12: a pair of 16-bit D/A (digital to analog) converters, an error amplifier, and a MOSFET driver stack. When a new scanner position is required, the drive D/A is updated, and it

drives the error amplifier. The second input to the error amplifier is the analog value of the current motor position. Whenever the inputs to the error amplifier are unbalanced, it provides the correction signal necessary to rebalance the system. This local closed loop is necessary as it will correct for small variations in scanner motor performance.

The MOSFET driver stack will be a quasi-complementary push-pull pair. This allows symmetrical drive and oppose characteristics but also allows the use of very low on-resistance N-channel FETs. The maximum average power dissipation from the motor load will be 0.5 Watts given a motor efficiency of 50%, a maximum load of 50 grams moved 35 mm in 50 milliseconds, and 50% duty cycle (worst case). The pair of scanners, together with analog drive and positioning electronics, should dissipate 2 to 3 Watts, which is easily handled with proper package thermal design.

The aperture plate design and fabrication are important for efficient scanner function. Thickness is a key aperture plate characteristic. The aperture plates must be less than 75 μm thick and move within 50 μm of one another. Various aperture materials will be evaluated. These include sheets of bare aluminum, anodized aluminum, teflon coated aluminum, chrome glass, and steel. 75 μm sheets are available and may be acceptable material if the crossed apertures never touch in high speed operation. If apertures touch while moving, it may be necessary to harden the surface and/or make it slippery by use of appropriate surface coatings. Glass sheets vacuum coated with metal have the advantage that the thickness of the coatings can be only a few μm thick, so that depth of field problems can be minimized. The mass of the glass, however, becomes a design issue and may limit the speed of operation. To guide the experimental effort, a mechanical design, including finite element modeling of apertures in motion, should be completed using NASTRAN simulation.

Considerable effort should be put into designing and building a package for holding a pair of scanners back-to-back with the plates very close together. The package must allow quick and simple adjustment of scanner separation and parallelism. This is a three degree of freedom positioning problem, but the amount of adjustment required for each degree is small. A total separation adjustment range of about 75 μm and angular adjustment on the order of 2 degrees in each axis is required. Many mount schemes are possible, but a low-cost, compact solution must be found.

5.4 Subaperture Detector

The detector will be a photomultiplier tube because of the requirements for low noise, large area, high speed, and low cost.[18] In addition to meeting the necessary requirements, photomultipliers have the additional advantages of being a mature, well-understood, and well-characterized technology. Furthermore they have the operational advantage of not requiring active temperature stabilization and having sufficiently low room temperature dark current that they can be operated uncooled for this application. Figure 13 plots responsivity versus wavelength curves for a variety of commercial photocathodes. GaAs is an attractive photocathode, because it has 10 percent quantum efficiency from the deep UV out to a wavelength of 800 nm. Unfortunately it is currently available only in small area (less than 3 mm diameter) devices. The specific photocathode chosen depends on the wavelength of operation. In the 300 to 540 nm range the photocathode of choice is a bialkali with quantum efficiency between 10 and 30 percent depending on wavelength. From 540 nm to 650 nm various semitransparent multialkali photocathodes have 5 to 10 percent quantum efficiency. It is undesirable to operate at wavelengths beyond 650 nm, because of the low quantum efficiencies. From a detector quantum efficiency viewpoint, it is most desirable to operate at as short a wavelength as possible, which is exactly the opposite direction as atmospheric transmission and sky background.

5.5 Array Electronics

The overall design philosophy is to build a modular, functionally partitioned system. The potential complexity of a full-scale system requires that testability and repairability be given the highest priority in the design process. Modules can be quickly interchanged allowing problems to be isolated and repaired with a minimum of system downtime. A modular approach is required for a "scaleable" system. A general description of the subsystem modules follows.

In a truly scaleable electronics system the need exists for the scaleable intervals to be either autonomous or easily interfaced with. The acquisition system requires synchronization of all the receiver and preprocessing elements, making a distributed control system desirable. The acquisition unit will utilize a controller subsystem to provide synchronization and operational instructions to the receiver modules. The controller must be flexible and easily reprogrammable to allow a variety of system configurations.

SPARTA, Inc. has developed a control processing (CP) system utilizing the Analog Devices ADSP2100 Digital Signal Processor as its processing engine. The ADSP2100 is capable of executing 25 million instructions per second. The ability to fetch multiple operands per operating cycle, plus multiple levels of interrupt

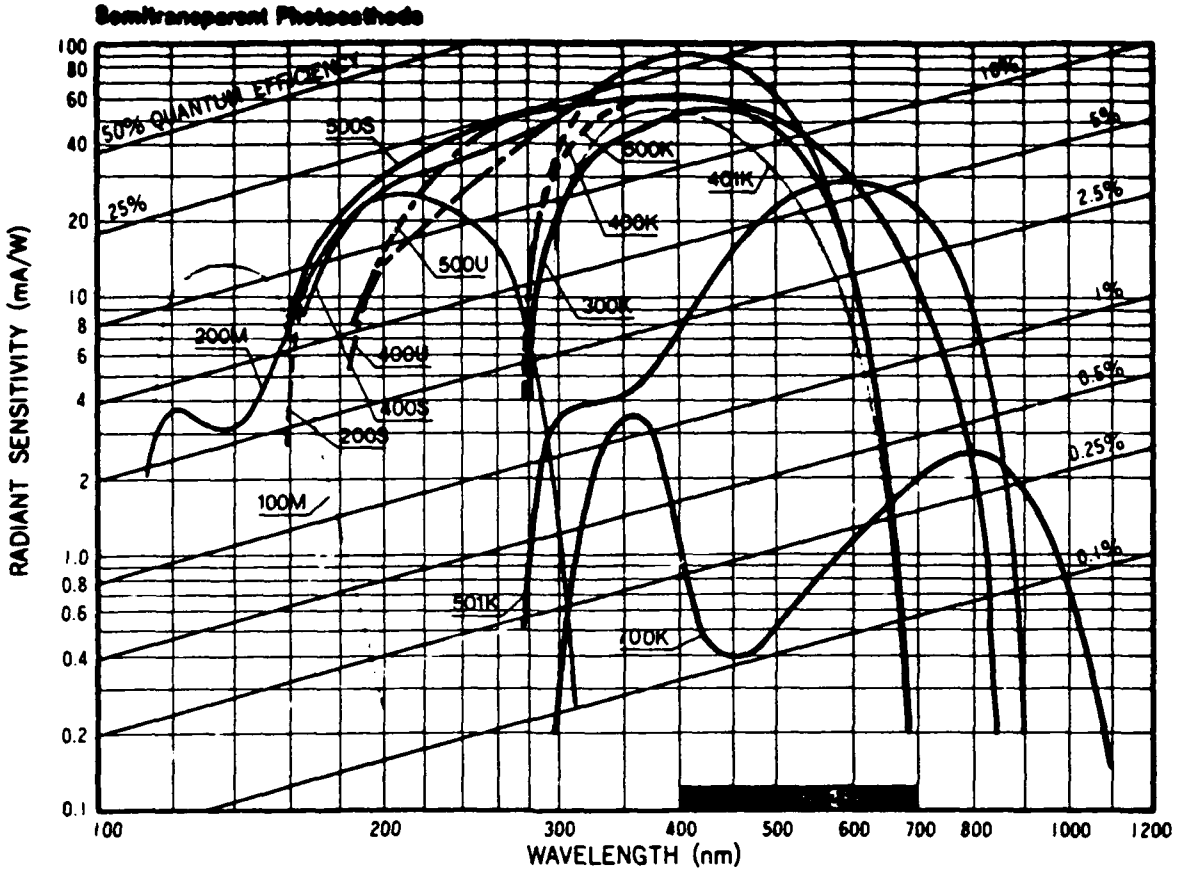

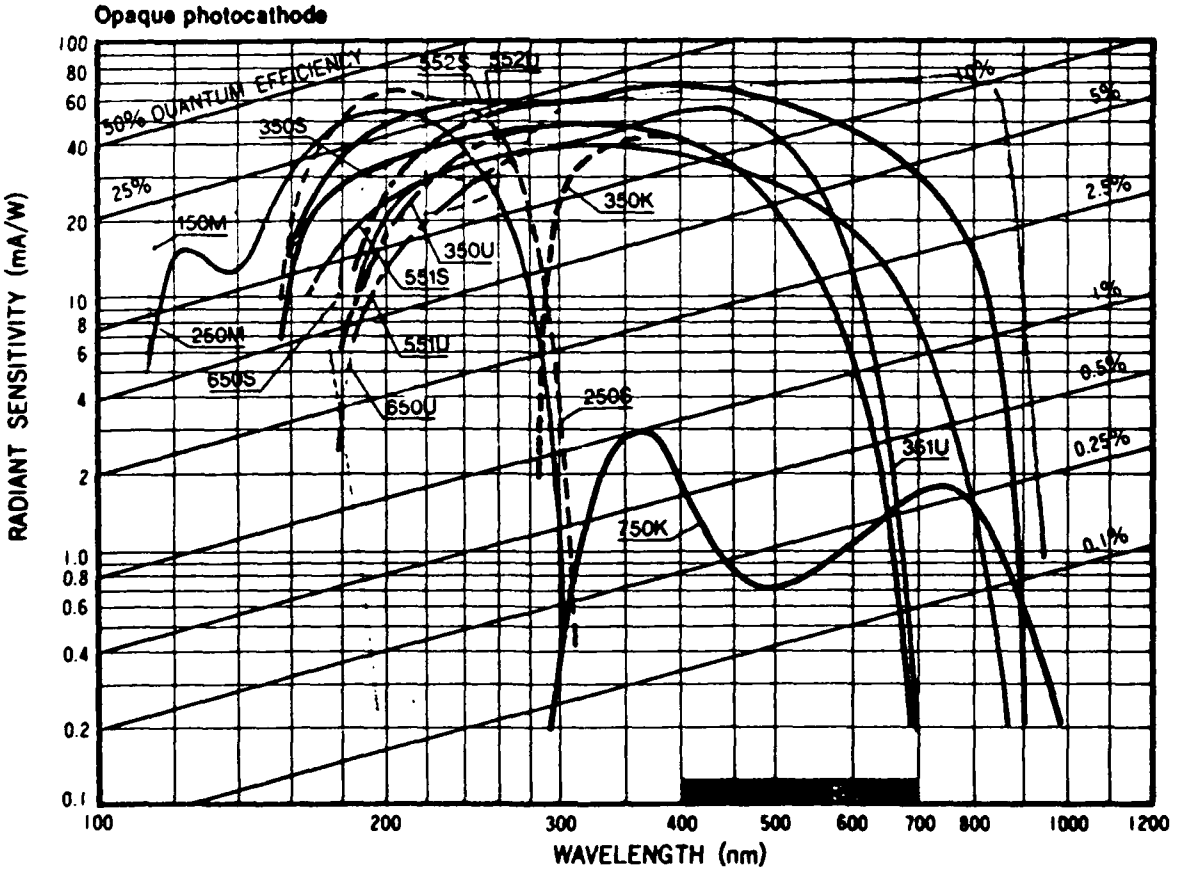

Figure 13. Responsivity versus wavelength for commercial photocathodes[19].

handling, contribute to the power and flexibility of this processor element.

Functionally, the controller subsystem will operate as follows. During idle time, the controller will be engaged in a "housekeeping" program which will perform a variety of built-in test routines enhancing the reliability of the system. If at any time during these test routines an interrupt is generated by the host system, the control processor immediately puts itself into a run condition and jumps to the synchronization and control routines. The interrupt handling overhead is one processor cycle (80 ns) and the run code will take a maximum of 5 cycles (400 ns) to invoke. The interrupt delays are constant and will not contribute to system timing errors.

The runtime operating system is triggered by the host-generated data pulse indicating the laser illumination pulse. Once the laser on pulse is detected, the CP enters the synchronization portion of its program. This utilizes a programmable delay generator in conjunction with a countdown program to range gate the receiver elements. The programmable delay generator divides the main clock (80 ns pulses) into 256 equal parts. Timing resolution on the order of 5 ns can be achieved with this method. Synchronization accuracy will also be within 5 ns throughout the receiver system. After the CP has completed the tasks of synchronizing the receiver integrators, it will direct the digitization and data multiplexing tasks, collecting the receiver data for processing. Host interfaces and I/O handlers will allow the maximum reliable data transfer rates possible, making the system laser repetition-rate-limited for raw data collection.

The receiver acquisition subsystem (RAS), illustrated in Figure 14, is a critical portion of the electronics. Its design must offer reliability and low cost since it is replicated for each subaperture in the receiver. The acquisition system integrates the receiver output during a tightly controlled time slice or window. This integrated signal is amplified and then digitized for later processing. The received signal-to-background noise performance is dependent on proper timing of the receiver integration window relative to the round trip time of flight for the target illuminating laser pulse.

The primary receiver element will be a photomultiplier tube with a gain in the range of 10^5 to 10^6. Assuming a minimum photon flux of 10 photons/subaperture, quantum efficiency of 10% and a 100 ns time window, the output current of the PMT will be approximately 1 microampere (μA). The PMT will be followed by a current amplifier to ensure adequate signal levels at the integrator. A current gain of 100 is required to allow a 100 pF integration capacitor. This size is useful because it is large enough that switch and stray circuit capacitances will have minimal effect. Switching and reset noise components will then be negligible error sources.

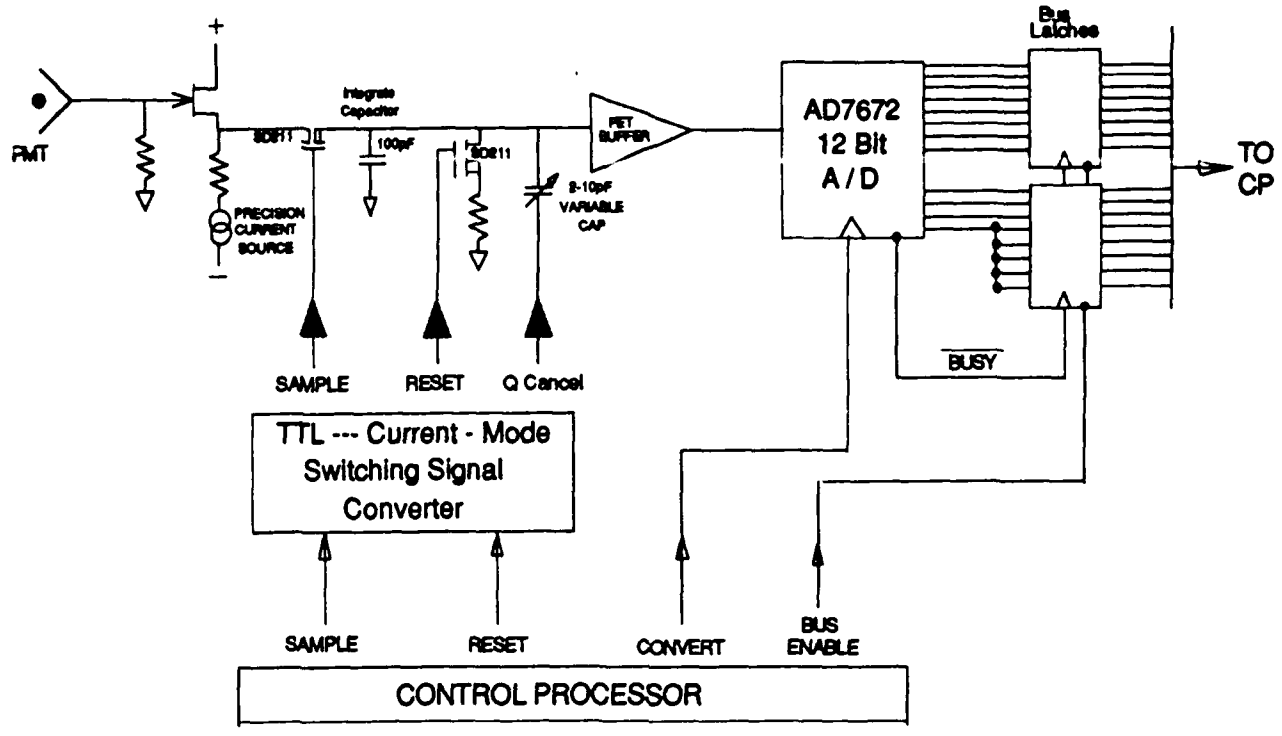

Figure 14. Receiver acquisition subsystem.

The operational PMT output dynamic range is assumed to be 1000:1. The maximum signal voltage allowed will be ±4 volts (allowing the use of ±5 volt power supplies, which will keep power dissipation low). This means a single photon event signal generates approximately 10 millivolts (mV).

Discharging the integration capacitor completely while minimizing noise contributions from the reset switches requires slow rise and fall times to the reset switch and a low impedance discharge path to a noise-free ground reference. Careful use of ground-planes in the circuit layout and using current-source based switching signals will ensure good noise performance from the integration electronics. The design goal is to maintain an integrator noise contribution error less than 100 μVolts, peak-to-peak, at the output. Timing and synchronization of the integrator is handled by the CP described previously.

The Analog to Digital (A/D) conversion will be handled by an Analog Devices AD7672 12-bit A/D converter. The RAS integrator acts as a sample/hold with a very low droop rate (less than 10 μV/μS). In the 10μS conversion time required by the AD7672, the held value will change by less than 0.1 LSB (least significant bit). The analog noise is on the order of 0.1 LSB, giving this system very good A/D conversion performance.

The output of the A/D converters will be latched into a bus transmitter. The output drive control of this transmitter will be addressed by the CP, putting the data onto the processor bus for further manipulation. A digital data multiplexer (mux) is created by having the output latch from each subaperture respond to a unique address, but driving a common data bus. A digital mux is preferable to an analog mux primarily for noise performance reasons. The mux will be designed to handle subaperture data at the maximum data rate determined by the product of the number of subapertures and the maximum laser repetition rate. A 4000 element system used with a 100 Hz rep rate laser will supply data at 400,000 samples per second, which can be readily accommodate with standard low cost digital circuitry.

5.6 Receiver Packaging

Many multi-aperture receiver concepts fail on paper when designers contemplate packaging the hardware into a two-dimensional array containing thousands of subapertures. To avoid such pitfalls, SPARTA established the following guidelines for evaluating candidate array packaging schemes. A viable design must be:

1) *Repairable* - Removal and replacement of a failed subaperture must be possible without disturbing the alignment or operation of the entire array.

2) *Adjustable* - Adjusting subaperture-to-subaperture spacing must not involve a complete redesign of the packaging hardware. Specifically, adjusting the spacing two or three times over the lifetime of the hardware must be accommodated in the packaging design.

3) *Steerable* - An array of four thousand subapertures must be coarsely steered to the appropriate azimuth and elevation angle *without* requiring a seven meter wide tracking mount!

4) *Expandable* - The array must be expandable in stages (e.g. 16×16, 32×32, 64×64, 128×128) without requiring any redesign or retooling of in-place mechanical hardware.

5) *Testable* - Any subaperture in the array must be removable for testing purposes without disturbing the operation or alignment of the entire array.

6) *Mechanically Stable* - Once the array is coarsely steered to within about one degree of its nominal imaging angle, the packaging hardware must maintain a 0.25 milliradian (rms) pointing stability for each subaperture over a period of one hour operation.

It was decided that the conditions of steerability and expandability (items 3 and 4) provided a compelling argument to break up the large array into individually

steerable, sixty-four subaperture subarrays as shown in Figure 15. Each of these subarrays would contain a coarse pointing mount, mechanical hardware to mount sixty-four subapertures in an 8×8 arrangement, cabling harnesses to supply power and signal paths, and local electronic digitizers, data buffers and control processors to service the subarray.

Any real subaperture contains a finite aperture area and hence does not point sample the speckle pattern. Thus, each subaperture averages the speckle intensity over its spatial extent and degrades the speckle pattern estimate.

The effect of array fill factor on the modulation transfer function (MTF) has been analyzed by a simple model which assumes that point illumination (i.e., delta function) enters a subaperture that has a fractional fill factor of (a) and this illumination generates crosstalk of fractional strength (b) in adjacent subapertures as shown in Figure 16. In speckle imaging, the effective MTF is the square of the Fourier transform, because a squaring operation is used to compute the autocorrelation of the intensity image. Thus the MTF is

$$MTF = [a\ \mathrm{sinc}(a\xi)[1 + 2b\cos 2\pi a\xi]]^2.$$

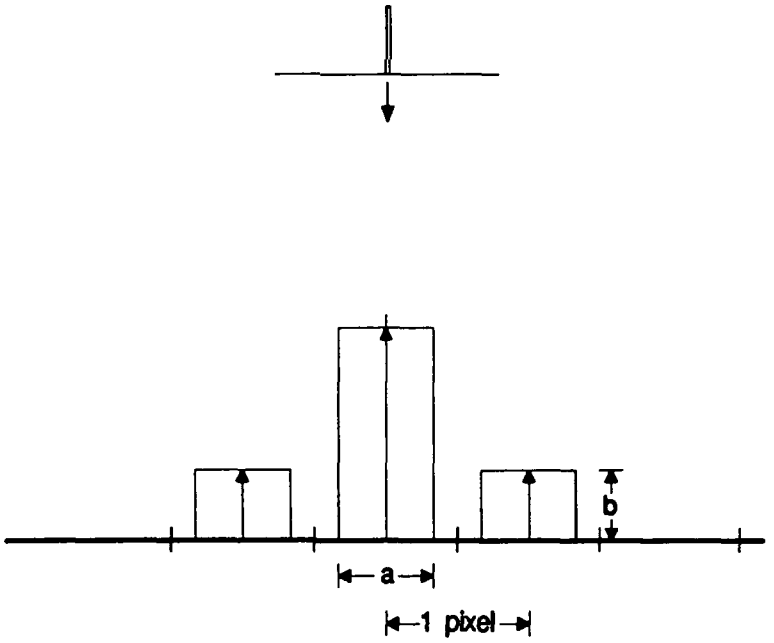

Figure 16. Point spread function model.

Earlier work[20] plotted families of MTF curves for a variety of fill factors and PSF sidelobe heights. Figure 17 plots MTF curves for varying linear fill factors, where no sidelobes are present. The straight line for a=0 represents point sampling.

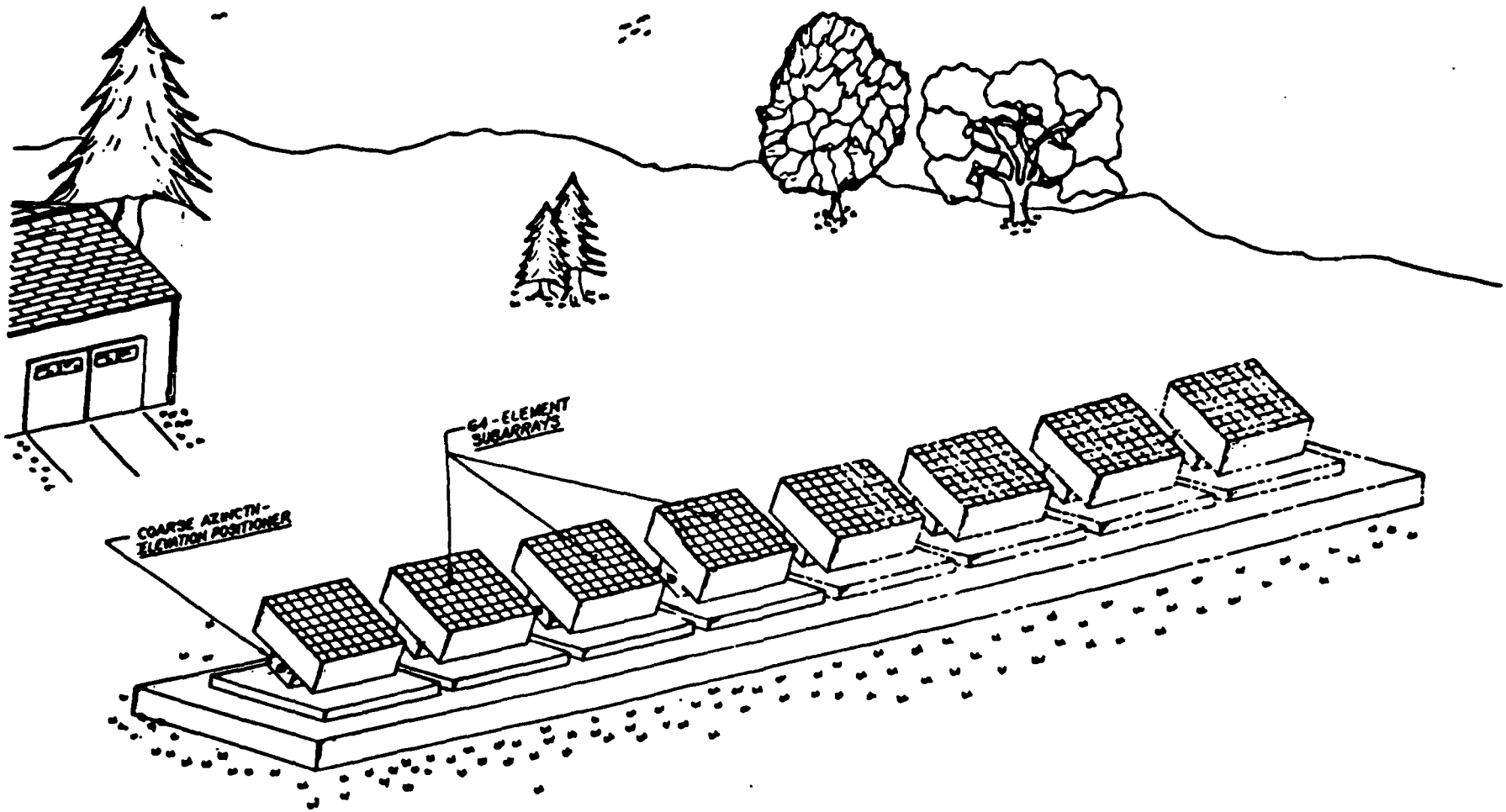

Figure 15. Concept sketch showing a possible multiple aperture imager deployment.

These curves illustrate that a tradeoff between MTF and SNR must be made, since the perfect MTF from point sampling would not actually collect any photons! A linear fill factor of 50 percent appears to be a reasonable choice, since MTF effects can be corrected (at least for high signal levels) even at the Nyquist limit, while a reasonable number of photons are collected. Consequently, the strawman receiver requirements specify a 5 cm diameter subaperture collection optic and a subaperture-to-subaperture spacing of 10 cm.

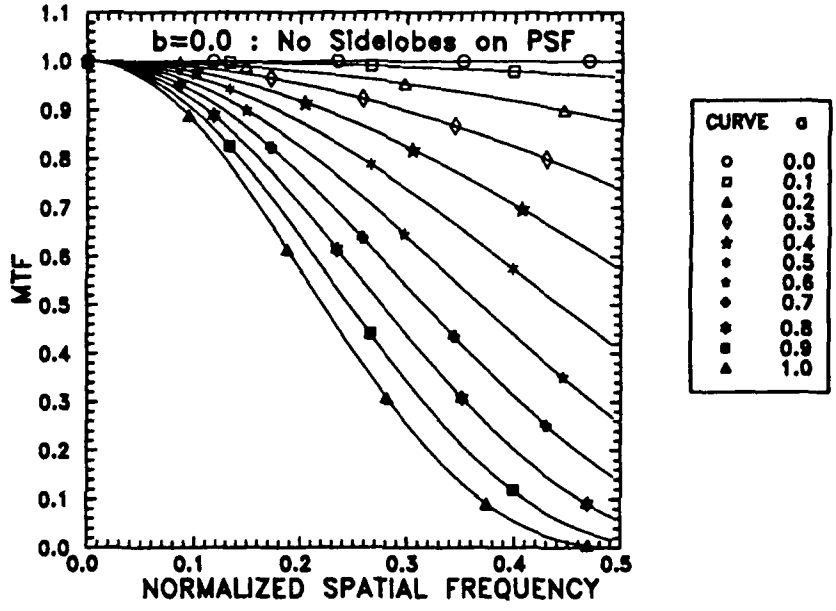

Figure 17. MTF as a function of subaperture fill factor.

The proposed mechanical structure is illustrated in Figure 18. This overall approach can pack subapertures together at a minimum center-to-center spacing equaling the collection lens diameter plus about 25 mm. Consequently, it will accommodate the baseline design of 5 cm diameter subapertures spaced 10 cm apart. A metal base plate fabricated using aluminum, carbon composite laminates, or some other lightweight, low-cost, and stiff material will serve as the interface to a coarse azimuth-elevation gimbal. It will also act as the platform upon which additional mounting hardware is placed. A series of vertical support plates will be attached to the baseplate using a number of identical angle brackets as shown. These vertical plates will be fabricated from the same material used for the base-plate, insuring matched thermal expansion properties. All vertical plates (eight per subarray) will be identical in design to facilitate low-cost manufacturing. The interfaces between the angle brackets, vertical plates and baseplate will be secured using dowel pins and screw fasteners. Consequently, the vertical plate spacing

can be changed by simply drilling, reaming, and tapping a series of holes in the baseplate. No complex milling or machining will be required.

Finally, subapertures will be fastened to the vertical plates using dowels and screws as shown in the figure. Once again, subaperture spacing will be defined by a series of holes, not complex machined features. An eight-subaperture column will form an integrated sub-unit, complete with a secured cable harness. This sub-unit will be removable without disturbing the alignment or operation of the remaining columns in a subarray. Furthermore, a malfunctioning sub-unit, once removed, could be tested, realigned, repaired, etc. on custom test fixtures. This modularity addresses the repairability, adjustability and testability guidelines listed as items 1, 2, and 5 above.

A conceptual design for individual subaperture packaging is shown in Figure 19. The lens, scanner, photomultiplier tube, etc., will each be held in square mounting blocks. A single mounting block design may be useable for both the lens and the scanner, since each requires a large hole for optical clearance and tapped holes for securing the components into the blocks. These mounting blocks will locate inside an extruded or mass-produced, U-shaped channel. These considerations lead to a potentially low-cost subaperture package that can be sealed and mounted to the vertical subarray plates using a metal top plate as illustrated in the figure.

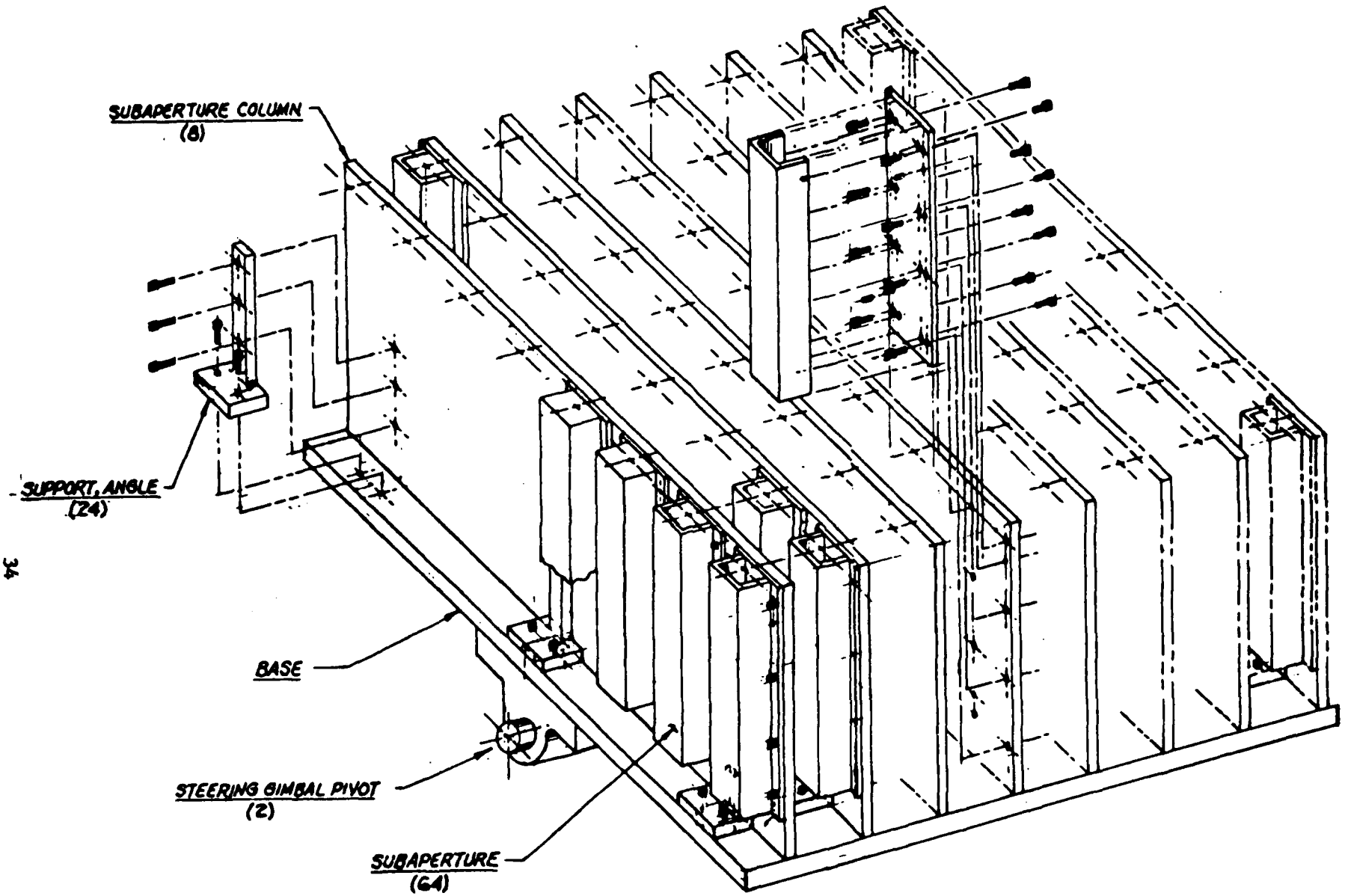

Figure 18. Modular packaging of subapertures.

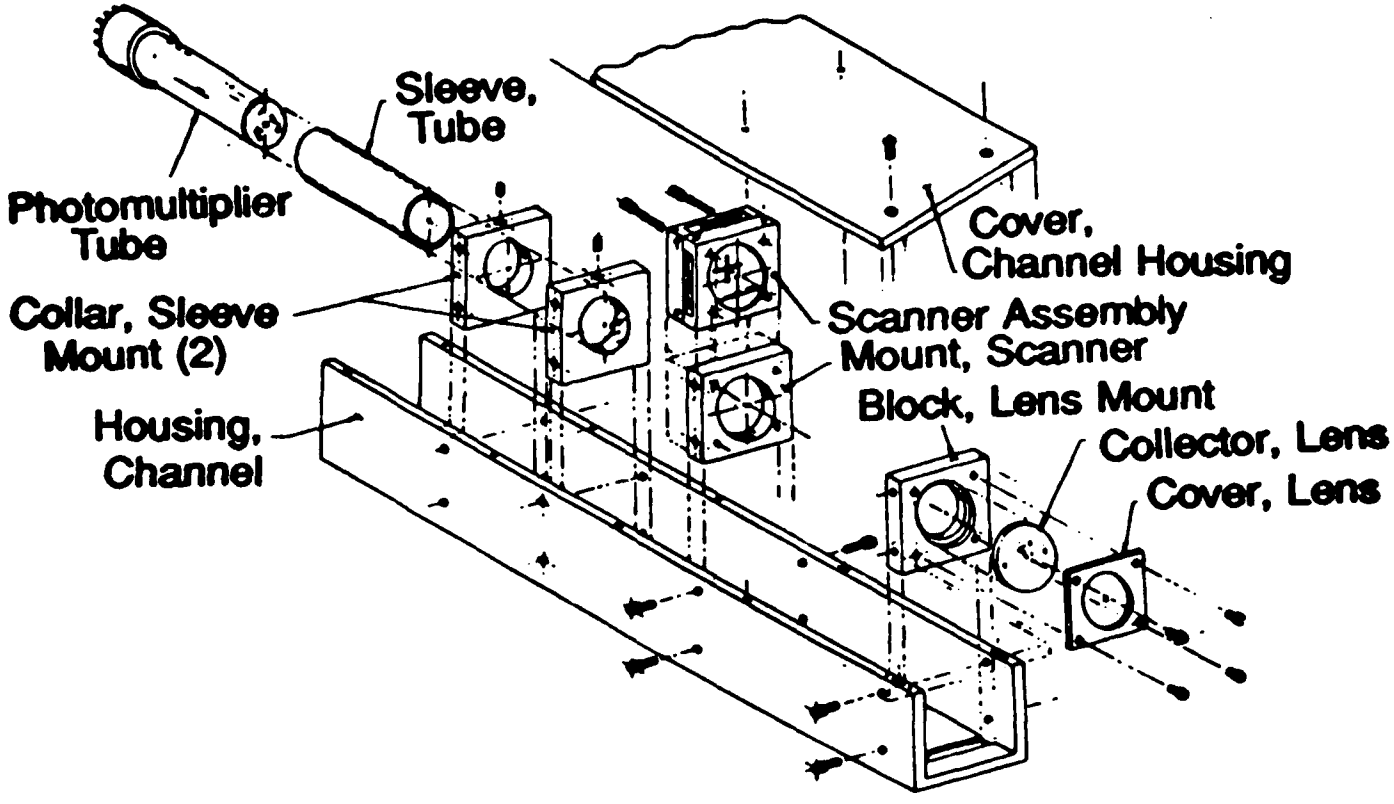

Figure 19. Exploded view of a subaperture.

6 Receiver Performance and Cost

This section addresses Task 4 of the Phase I Statement of Work.

The design discussed in the last section meets all the receiver requirements presented in Table I. The cost of achieving each required parameter will be discussed in turn.

The 20 degree full FOV requires a custom lens to achieve flat field conditions, but it should be a straightforward design. The dynamic range of 1000 can be met with a part and well designed under electronics. A full field slew rate of 50 milliseconds can be handled by a custom-built linear motor.

The dark current requirement is easily met by the high-gain and low noise characteristics of PMTs. The Hamamatsu R1705 tube is a 38 mm diameter device with a maximum anode dark current of 10 nA, which is 6000 electrons over a 100 ns integration time. The current amplification of the R1705 is 5×10^5 so that the maximum dark current corresponds to about 0.01 photoelectrons at the cathode, which is two orders of magnitudes better than required.

The cost of a Phase III array is linearly proportional to the number of subapertures. A 64 by 64 element array contains 4096 subapertures, so that the assembled cost per subaperture must be approximately $1200 to keep the array cost to $5M. Each subaperture contains optical, mechanical, and electrical components which must be designed, fabricated, and assembled. Table V is a list of major subaperture components and their estimated unit costs in quantities of 100. The purpose of this table is to show that component costs are in the right ballpark. Mission requirements related to field-of-view will greatly affect the actual system cost. The component costs for a system with 4000 subapertures will be significantly lower, but a careful volume cost estimate cannot be done until a prototype unit has been fabricated. These cost estimates do not include assembly time. The system cost also will include the "eggcrates" which contain wiring connectors and wiring to hold an 8 by 8 array of subapertures. A prototype eggcrate will be designed, built, and tested with a pair of subapertures to accurately estimate system cost.

Table V. Cost estimate of major subaperture components in quantity 100.

COMPONENT	ESTIMATED COST
PMT detector	300
High voltage supply	40
Socket/dynode chain	15
Current amplifier	12
Discrete component integrator	40
12 bit 200 KHz A/D	60
A/D logic and digital MUX interface	10
Position sensors (2 axes)	100
Scanner control/electronics	200
Circuit boards	30
Scanner assembly and apertures	300
Collection lens	100
Optical spectral filter	20
Optical polarizer	20
Housing	30
TOTAL	$\approx$ \$1300

7 Conclusions

The Phase I work completed all its objectives by answering the three questions posed in the Phase I proposal. These questions were as follows:

1. What are the performance requirements for a multiple aperture receiver designed to operate in a ground-to-space imaging experiment?
2. Can a receiver be designed using existing component technologies to meet these requirements and, if so, what would the design look like?
3. If a suitable design exists, are the risk and cost associated with its implementation low enough to be practical?

Firstly, receiver performance requirements were identified for a strawman ground-to-space multiple aperture imager (MAI) experiment. Secondly, a concept for a practical, low-cost subaperture receiver was identified by eliminating a large number of competing schemes. Thirdly, a candidate subaperture array packaging scheme was identified which potentially accommodates receiver testing, adjusting, and repairing while supporting coarse array steering, easy array expansion and long-term mechanical pointing stability.

The Phase I study has concluded that a practical subaperture is feasible and can be built with existing technology.

8 References

1. P. D. Henshaw and D. E. B. Lees, "Electronically Agile Multiple Aperture Imager," in *Digital Image Recovery and Synthesis*, SPIE Proceedings **828** 16-21 August 1987, San Diego, CA, pp. 134-139.
2. R. F. Dillon, D. E. B. Lees, P. D. Henshaw, and J. R. Jones. "Multiple Aperture Imager Development Final Report," Contract No. DNA001-87-C-0155, (in preparation).
3. Multiple Aperture Imager Component Development, ONR contract N00014-88-C-0518.
4. D. E. B. Lees and P. D. Henshaw, "A New Method for Direct Image Recovery From Speckle Patterns," presented at 1989 Annual Meeting of the Optical Society of America in Orlando, Florida, October 15-20.
5. D. E. B. Lees, "Improved Autocorrelation Zero-Lag Estimation In Multiple Aperture Imaging Systems," IRIS Active Systems Conference, Boulder Colorado, October 18-20, 1988.
6. P. D. Henshaw and D. E. B. Lees, "Multiple Aperture Imaging SBIR Phase I Final Report," SPARTA LTR86-13, Lexington, MA (30 December 1986).
7. P. S. Idell and J. R. Fienup, "Imaging Correlography with Sparse Collecting Apertures," SPIE Proceedings **828** 16-21 August 1987, San Diego, CA, pp. 140-148.
8. P. D. Henshaw, "Multiple Aperture Imaging System Construct," from *Optical Discrimination Study (Classified)*, 9 November 1984, Vol. IV-A, pp. 119-130.
9. Ibid.
10. B. Lyot, Compt. Rend. Acad. Sci., **197** 1593 (1933).
11. R. W. Engstrom, Photomultiplier Handbook, (RCA, Lancaster, PA, 1989).
12. Photomultiplers, (Thorn LSMI, 1986).
13. S. Soltesz, RCA, Private communication on silicon avalanche photodiodes, 1989.
14. A. W. Lightstone and R. J. McIntyre, Photon counting silicon avalanche photodiodes for photon correlation spectroscopy, Presented at OSA Topical Meeting on photon correlation techniques and application, May 30-June 2, 1988, Washington D.C.
15. EG&G Photon Devices, Photodiodes, (EG&G, Salem, 1989).
16. Photometrix, Inc., Sales Literature, Tuscon, AZ, 1990.
17. E. H. Eberhardt, The modulation transfer function of microchannel and fiber optic plates, Technical Note 126, (ITT, Ft. Wayne, 1980.)

18. Ibid.
19. Hamamatsu Photonics K.K., Electron Tube Division, January 1988.
20. Ibid.